Submitted to Physical Review

UCRL-19510
Preprint

cy. 2

A STUDY OF THE LOW ENERGY TRANSITIONS ARISING FROM THE PROMPT DEEXCITATION OF FISSION FRAGMENTS

RECEIVED
LAWRENCE
RADIATION LABORATORY
DEC 5 1969
LIBRARY AND
DOCUMENTS SECTION

R. L. Watson, J. B. Wilhelmy, R. C. Jared,
C. Rugge, H. R. Bowman, S. G. Thompson, and J. O.
Rasmussen

November 1969

AEC Contract No. W-7405-eng-48

TWO-WEEK LOAN COPY

This is a Library Circulating Copy which may be borrowed for two weeks. For a personal retention copy, call Tech. Info. Division, Ext. 5545

UCLR-19510
cy. 2

LAWRENCE RADIATION LABORATORY
UNIVERSITY of CALIFORNIA BERKELEY

DISCLAIMER

This document was prepared as an account of work sponsored by the United States Government. While this document is believed to contain correct information, neither the United States Government nor any agency thereof, nor the Regents of the University of California, nor any of their employees, makes any warranty, express or implied, or assumes any legal responsibility for the accuracy, completeness, or usefulness of any information, apparatus, product, or process disclosed, or represents that its use would not infringe privately owned rights. Reference herein to any specific commercial product, process, or service by its trade name, trademark, manufacturer, or otherwise, does not necessarily constitute or imply its endorsement, recommendation, or favoring by the United States Government or any agency thereof, or the Regents of the University of California. The views and opinions of authors expressed herein do not necessarily state or reflect those of the United States Government or any agency thereof or the Regents of the University of California.

A STUDY OF THE LOW ENERGY TRANSITIONS ARISING FROM THE PROMPT DEEXCITATION OF FISSION FRAGMENTS†

R. L. Watson*
Lawrence Radiation Laboratory,
University of California, Berkeley, California and
Department of Chemistry and Cyclotron Institute
Texas A&M University, College Station, Texas 77843

and

J. B. Wilhelmy, R. C. Jared, C. Rugge, H. R. Bowman, and S. G. Thompson
Lawrence Radiation Laboratory
University of California, Berkeley, California

and

J. O. Rasmussen‡
Lawrence Radiation Laboratory,
University of California, Berkeley, California and
Department of Chemistry
Yale University, New Haven, Connecticut

Abstract: A four dimensional experiment has been performed in which the energies of coincident complementary fragment pairs, internal conversion electrons, and K x-rays emitted as a result of the spontaneous fission of ^{252}Cf were recorded event by event using a multiparameter analyzer. The fission fragment energies were used for mass identification and the x-ray energies supplied precise atomic number identification. The analysis of the conversion electron

†Work at University of California Lawrence Radiation Laboratory supported by the U. S. Atomic Energy Commission.
Work at Texas A&M University supported in part by the U. S. Atomic Energy Commission and the Robert A. Welch Foundation.

*Present address: Department of Chemistry and Cyclotron Institute, Texas A&M University, College Station, Texas 77843.

‡Present address: Department of Chemistry, Yale University, New Haven, Connecticut.

spectra has resulted in the assignment of numerous transitions to new isotopes, the determination of many transition half lives, and the procurement of limited information concerning multipolarities. It was concluded, based on the x-ray and conversion electron data, that most of the large number of observed low energy transitions associated with heavy fragments are attributable to odd-mass or odd-odd nuclei and that surprisingly little contribution to the low energy spectra is associated with even-even nuclei in the rare earth region. Low energy transitions in even-even nuclei were found to be more prevalent among the light fragments. Data are presented supporting the assignment of a high intensity 241 keV transition as the 2+ to 0+ transition in ^{110}Ru. An examination of this transition in terms of the energy predicted on the basis of rotational behavior and with regard to the systematics of neighboring even-even Ru isotopes reveals evidence which strongly suggests that ^{110}Ru belongs to a new region of stable deformation.

E | NUCLEAR FISSION ^{252}Cf fission products; measured $E_{(ce)}$, $I_{(ce)}$, $T_{1/2}(ce)$, $E_{(x)}$, $I_{(x)}$.

1. Introduction

Primary (pre-beta decay) fission fragments are interesting nuclear species because they contain large excesses of neutrons, are in states of moderately high nuclear excitation, and possess on the order of 8 to 10 units of angular momenta. Consequently, studies of their nuclear properties could lead to important new discoveries which are unique to this special class of nuclei. Furthermore, the ability to examine specific fragments as identified by their characteristic radiations would provide a powerful method whereby information pertaining directly to the fission process could be obtained.

Experimentally, detailed investigations of the deexcitation processes of primary fission fragments are extremely difficult. This is due to the fact that there is no way to study any one isotope without the interfering radiations from numerous others since many different products are formed in fission. Modern electronic devices and solid state radiation detectors, however, have now made possible multidimensional investigations in which the coincident radiations of fission fragments may be measured and correlated. By simultaneously measuring the gamma-ray energies and fission fragment energies associated with individual fission events, Bowman, Thompson and Rasmussen[1]) successfully demonstrated the capability of reducing the previously observed continuous gamma-ray spectrum from ^{252}Cf fission fragments into spectra displaying discretely resolved structure when sorted with respect to fragment mass. Following this experiment, Watson[2]) measured the spectra of internal conversion electrons associated with intervals of fragment mass and identified transitions with fragments of specific atomic numbers by comparing the observed electron line energies with the gamma-ray energies observed by Bowman[3]). These assignments, however, were very tentative because of the relatively poor

electron and gamma-ray energy resolution obtained in the two experiments. The mass and atomic number assignments were both estimated to be uncertain by ±1 unit.

In order to eliminate the uncertainty in the atomic number assignments, the present experiment was undertaken in which coincident K x-ray energies were also measured and recorded simultaneously with the electron and fission fragment energies using a multidimensional pulse height analyzer. The details of this experiment and the combined results of this plus those from the above mentioned study of Watson are reported here.

2. Experimental procedures

2.1 APPARATUS

The precise measurement of electron energies requires the elimination of any window for the electrons to penetrate that would seriously degrade the resolution obtainable with the spectrometer being used. In the present experiment, this restriction necessitated that the electron spectrometer (a lithium-drifted silicon detector of dimensions 1 cm x 2 cm x 3 mm) be located inside the fission chamber, imposing the further complication of devising a means of shielding the detector from interference by fission fragments, alpha particles, x-rays and gamma-rays. Conventional methods of shielding, such as placing the detector behind a lead collimator with a view of only a small portion of the fragment flight path, result in such a low detection geometry as to make any detailed study impractical. The problem was resolved by employing a magnetic steering device to guide the electrons around a 90° arc, away from the fission source, to a shielded detector. This steering device utilized the highly

convergent fringing field of a large electro-magnet where conditions were such that high transmission (14%) was attained with no dependence on electron energy. A detailed description of the design and operation of this device is given in ref.[4]). The electron detector and internally mounted FET were operated at liquid nitrogen temperature and gave an energy resolution of 2.5 keV FWHM for the 661 keV electron peak arising from the decay of ^{137}Cs.

A schematic diagram of the experimental arrangement is shown in fig. 1. A weightless amount of ^{252}Cf deposited onto a thin (~70 μg/cm^2) nickel foil by self transfer from a 10 μg source (which was collimated to 1/16 in.) was mounted between two phosphorus-diffused silicon fission fragment detectors. The fragment detectors were collimated to 15 mm in diameter and operated at -50°C. Directly below the fragment detector-source axis and centered at the symmetry plane of the magnet was located a lithium drifted silicon x-ray detector of dimensions 1/2 cm x 1/2 cm x 3 mm. This detector was mounted in a separate evacuated cryostat which was isolated from the main vacuum chamber by a 0.010 in. beryllium window. The detector and internally mounted FET were operated at liquid nitrogen temperature and gave an energy resolution of 0.75 keV FWHM at 14 keV.

The region of acceptance of electrons into the steering device was defined by two deflectors which prevented electrons emitted outside this region from reaching the electron detector (see ref.[4]). The fragment detector-source-deflector configuration used in this experiment was as follows: the ^{252}Cf source was mounted on one of the deflectors and positioned at a distance of 1 cm from the magnet symmetry plane. Fragment 1 detector was mounted 2 cm from the magnet symmetry plane on the same side as the source and fragment 2 detector was mounted on the other deflector 1 cm from the magnet symmetry plane on the other side. The source, fragment detectors and deflectors were

all mounted coaxially. Since the average fission fragment velocity is about 1 cm/nsec, this arrangement enabled us to observe only electrons which were emitted approximately 1 nsec after fission with a calculated time resolution of 1.7 nsec FWHM. Utilizing this same technique, Watson[2]) measured the spectra of electrons emitted at approximately 2 nsec after fission as well and used relative intensities of electron peaks appearing in the two measurements to determine transition half-lives.

2.2 ELECTRONICS

The complexity of this type of experiment stems from the fact that not only must the energies of electrons, fission fragments and x-rays evolving from the same fission events be individually measured and recorded, but also the event-by-event correlation must be maintained. The electronic system was assembled in such a way as to enable the following:

(a) The measurement and event-by-event analysis of

(1) Fragment 1-fragment 2-electron coincidences (type 1 events)

(2) Fragment 1-fragment 2- x-ray coincidences (type 2 events)

(3) Fragment 1-fragment 2-electron-x-ray coincidences (type 3 events).

(b) The optimization of energy and time resolution.

(c) The maintainance of electronic gain stability over long periods of time.

Pulses from the fission fragment detectors were amplified by standard low-noise preamplifiers while those from the electron and x-ray detectors were sent to special preamplifiers designed by Jared and Kilean[5]). The signals were then routed to linear amplifier systems via variable gain amplifiers. Zero crossover signals were generated in each system and were subsequently subjected to a fourfold coincidence requirement by means of which only events

for which two complementary fission fragments and an x-ray were detected within 100 nsec after a fission event,and an electron was detected within the time interval of 18 nsec to 180 nsec after the same fission event were recorded as type 3 events. (The large resolving time for electrons was needed because of the lengthy flight time required for the transmission of low energy electrons in the magnetic steering device). The fission fragment zero crossover signals were further subjected to a fast double coincidence requirement having a 50 nsec resolving time. Whenever an event occurred in which the fourfold and double coincidence requirements were satisfied, a gating signal was fed to a Nuclear Data multidimensional analyzer, which in turn analyzed the pulse-heights from the various amplifier systems. Other coincidence circuits were connected in such a way that triple coincidence events (type 1 and type 2 events) generated separate analyzer gates if the fission fragment double coincidence requirement was also fulfilled. Each of the pulse-heights associated with the various event types were digitized by a separate dimension of the analyzer and stored in the memory event by event, so that the order of the detector pulses was maintained. Each time the analyzer memory became full, the output was written on magnetic tape.

Since the fourfold coincidence counting rate was very low (~10 per minute) the experiment had to be run continuously for a period of approximately two months in order to obtain 1×10^5 type 3 events. To avoid any possible gain shifts that would alter the detector energy calibrations during the long operation periods, a digital-gain stabilizer system of the type described by Nakamura and LaPierre[6]) was incorporated into the electronic system. This unit continuously monitored distributions of selected events from each detector and maintained the first moments of these distributions in prescribed positions by feeding back to the variable gain amplifiers preceding the main amplifiers

the analog voltages corresponding to the differences in the number of pulses appearing above and below the pre-selected peak channels. The stabilizers were triggered by coincidence gates generated by each detector. The electron system was stabilized by monitoring the 277.6 keV gamma-ray of a ^{243}Cm source mounted directly behind the electron detector on the surface of a semi-conductor alpha detector. The stabilizer gating pulses were generated by requiring a double coincidence between gamma-rays detected in the electron detector and alpha particles detected in the alpha detector. Stabilization of the x-ray system was achieved in exactly the same way by monitoring the 59.5 keV gamma ray in coincidence with the alpha decay of ^{241}Am. The fission fragment systems were stabilized by monitoring the light-fragment distribution and gating was accomplished by means of the double coincidence requirement between fragments detected in detector 1 and fragments detected in detector 2. This also enabled the simultaneous recording of the double coincidence fragment distribution.

Every event which generated an analyzer gate was identified as one of the three event types or as one of the four types of stabilization events by a marker pulse. This marker pulse was sent to the fifth dimension of the multidimensional analyzer and identification of the different event types was accomplished by placing a count in the appropriate channel number.

2.3 DATA PROCESSING

Upon completion of the experiment, the data tapes were processed on a CDC 6600 computer. Basically this processing consisted of (a) separating the different event types, (b) sorting each event of the three event types and of the (double coincidence) fragment stabilization events into 2 amu intervals of mass by means of their coincident fission fragment pulse heights

(the details of the mass computation are given in the Appendix), (c) plotting the triple coincidence electron spectrum (event type 1), the triple coincidence x-ray spectrum (event type 2), the fourfold coincidence electron spectrum (event type 3), and the fourfold coincidence x-ray spectrum (event type 3) - associated with each interval of mass by Cal Comp plotter, and (d) plotting the various stabilization spectra for energy calibration purposes. After the triple coincidence and fourfold coincidence-electron spectra had been examined, further processing was carried out by placing "windows" on each observed electron peak and sorting out only those fourfold coincidence x-ray events which were in coincidence with events in the electron peak "window". These sorts, which will henceforth be referred to as "x-ray window sorts", were carried out for each mass interval in which the electron peak appeared.

3. Results

3.1 TRIPLE COINCIDENCE ELECTRON MEASUREMENTS

The triple coincidence electron measurements (type 1 events) of the present experiment were essentially identical to the 1 nsec measurements made previously by Watson. We therefore present here the more complete results of these earlier studies.*

The total electron spectra unsorted with respect to fragment mass are compared in fig. 2 for three experiments. The three sets of data were taken (a) with the fission source at the magnet symmetry plane, (b) with the fission source 1 cm from the magnet symmetry plane, and (c) with the fission source 2 cm from the magnet symmetry plane. With the source in these various positions, electron detection was restricted to those electrons emitted by fission

*The present measurements did, however, show that the electron peak energies determined in the earlier experiments were shifted down in energy by 3.0 keV. The results we report here have been corrected for this energy shift.

fragments which had traveled to within the distance intervals of 0 to 0.9, 0.1 to 1.9 and 1.1 to 2.9 cm from the fission source. Since these fission fragments travel with an average velocity of approximately 1 cm/nsec, the curves in fig. 2 represent the energy spectra of electrons emitted from fragments of all masses at the average times of (a) 0.4 nsec, (b) 1.0 nsec, and (c) 2.0 nsec after fission.

Clearly visible in the gross spectra of fig. 2 are well-defined electron peaks characteristic of the interval conversion of nuclear gamma-ray transitions. Specifically, peaks are seen at energies of 28, 36, 45, 93, 106, 121, and 153 kev. Furthurmore, the structure displays a rapid increase in intensity and complexity with decreasing energy in accordance with the well-known dictates of the internal conversion process. Using the total yields of electrons (summed over all energies) in the three time intervals represented by the spectra in fig. 2, a decay curve was constructed and found to be crudely analyzable in terms of a two component decay. The resulting half-lives of the two components were 0.17 nsec and 2.6 nsec.

Mass sorted spectra are shown in fig. 3 for three heavy fragment mass intervals and in fig. 4 for two light fragment mass intervals. They were obtained by sorting the data shown in fig. 2(b) (i.e. data from the experiment in which the source was 1 cm from the magnet symmetry plane) with respect to the masses of the coincident fragments. It is quite evident that sorting with respect to mass has indeed accomplished the desired effect of decreasing the complexity of the spectra to the point of making possible energy and mass determinations of many transitions.

Although the sorting process has greatly simplified the electron spectra, it has by no means reduced them to the realms of simple analysis for no

restrictions have been placed upon the atomic numbers of nuclides contributing to the spectra. Therefore each spectrum contains possible major contributions from at least three different elements. Moreover, complexity also arises from the fact that each electron peak is spread over 5 to 6 mass intervals due to the dispersion involved in determining a fragment mass. (An accurate determination of the experimental mass resolution is discussed in section 3.3.) A number of the electron peaks in figs. 3 and 4 have been labeled alphabetically for use here in showing specific K and L conversion lines and for use later in demonstrating the correlation between these spectra and the gamma-ray measurements of Bowman.

Two spectra for the mass interval 145 to 147 - - one with the source 1 cm from the magnet symmetry plane ($\bar{t}$ = 1 nsec) and the other taken with the source 2 cm from the magnet symmetry plane ($\bar{t}$ = 2 nsec) - - are compared in fig. 5. It can be seen that the relative intensities of several of the peaks change markedly in these two spectra due to their different rates of decay. A detailed analysis of the relative intensities of peaks appearing in the 1 nsec and 2 nsec experiments has enabled the determination of numerous transition half-lives with an estimated accuracy of ± 20%.

The aforementioned gamma-ray investigations of Bowman were basically similar to the present triple coincidence electron measurements in that the gamma-rays were detected in coincidence with the fission fragments (using a lithium drifted germanium detector), the fragment energies were measured and recorded with the energies of the coincident gamma-rays, and the data were processed and sorted in a similar fashion. Spectra were taken with the gamma ray detector positioned at 90° and at 0° - 180° with respect to the fragment flight path. Three gamma-ray spectra obtained by Bowman at 90° to the fragment flight path are shown in fig. 6 for the same mass

intervals as the electron spectra of figs. 3 and 4. Since in the gamma-ray experiments there was no way in which detection could be limited to only those gamma rays emitted by a selected member of each fragment pair, these spectra contain gamma-ray lines from both the light fragments and the coincident heavy fragments belonging to the mass intervals specified in the figure. In order to demonstrate the consistency between the electron data and the gamma-ray data, the approximate energies of gamma rays giving rise to the labeled K and L conversion electron lines in figs. 3 and 4 were calculated from the binding energies of the most probable charge elements. The resulting gamma-ray energy positions are indicated by arrows and identified by the letters of the corresponding electron peaks in fig. 6. As can be seen, excellent agreement is obtained in most cases. A complete compilation and comparison of the 1 nsec electron spectra and of the 90° and 0 - 180° gamma-ray spectra obtained in these earlier studies may be found in ref.[7]).

In the analysis of the electron spectra, account had to be taken of the energy shift and broadening of the electron peaks due to the fact that the electrons were emitted from fission fragments traveling with relatively high velocities. Utilizing the calculated dependence of the electron peak widths on energy and fragment velocity, a Gaussian least squares fitting program was constructed for the computer analysis of these spectra. The program operated in such a way that any number of peaks up to and including ten, each individually specified by a width consistent with its energy and associated fragment velocity, could, in combination, be varied in their intensities and first moments to obtain the best possible fit to the experimental data. An example of this analysis is given in fig. 7 for

the electron spectrum associated with the mass interval 145 - 147. As can be seen, the low energy region of this spectrum is extremely complex. Also observable is the manner in which the peak widths increase with energy. In this spectra they vary from 4.0 kev FWHM at 19 kev to 7.4 kev FWHM at 161 kev.

There are, of course, always a number of uncertainties involved in fitting data of this sort since regions composed of more than one peak may frequently be fit equally well, from a statistical point of view, by several combinations of peaks. In the present situation, however, a rigid constraint exists in the requirement that each individual peak of any combination of peaks exhibit a distinct behavior as a function of mass. Specifically, any given peak must display a constant first moment over all mass intervals in which it appears and (as will be discussed further in section 3.3) its intensity when plotted as a function of mass must be roughly Gaussian in shape with an average standard deviation of approximately 2.5 amu.

As already mentioned it was necessary to correct the electron peak energies obtained from the computer analysis for the small energy shifts imparted to the electrons due to the motion of the fragments. These upward energy shifts varied from 0.2 kev shift for 20 kev electrons emitted from mass 160 fission fragments to 0.8 kev shift for 200 kev electrons emitted from mass 100 fission fragments. Furthurmore, in calculating gamma-ray transition energies based on the conversion electron peak energies, account had to be taken of the increase in electron binding energies due to the high states of ionization of the fission fragments. Calculations of the shift in K electron binding energies in highly ionized atoms have shown the shift to be a nearly constant 0.9 kev over the range of elements produced in fission[8]).

By summing the number of events in each electron spectrum over energy, the electron yield as a function of mass was obtained and is shown in fig. 8 for the two approximate time intervals of 0.1 to 1.9 nsec and 1.1 to 2.9 nsec after fission. These curves include only those electrons of energies between 10 and 180 kev. The yields are seen to be quite sharply peaked at mass 108 and mass 150. Other noteworthy features include the extremely low yield observed near symmetric fission products, the slight discontinuities near masses 114 and 141 and the sudden drop in yield after mass 151. Several previous studies[9,10,11] of x-rays emitted in fission have revealed very nearly the same structure in the x-ray yield curves. These various authors have all discussed the significance of these features and therefore we shall not comment furthur on them here.

3.2 TRIPLE COINCIDENCE K X-RAY MEASUREMENTS

Analysis of the mass sorted x-ray spectra was carried out using an x-ray peak fitting procedure which enabled the unfolding of each complex x-ray spectrum. In this way the intensities of x-rays associated with intervals of fragment mass were obtained for each element. Using this information, most probable charge and mass values for the emission of K x-rays were determined and their relation to the primary fragment distribution was investigated. An examination of the effect of total kinetic energy on the x-ray distribution was also carried out. Since the results of these measurements are not pertinent to the interests of the present paper, they will be reported in a separate publication[12]).

3.3 FOURFOLD COINCIDENCE K X-RAY AND CONVERSION ELECTRON MEASUREMENTS

As mentioned in section 2.3, the fourfold coincidence data was used to make "x-ray window sorts" for the purpose of determining the atomic number

of the nuclide responsible for any given electron peak. Examples of the results of this analysis on an electron spectrum for the light fragment mass interval 107 - 109 are shown in fig. 9. The energy intervals labeled alphabetically in the electron spectrum delineate the "windows" used in the "x-ray window sorts". The x-ray spectra shown in fig. 9 were obtained by sorting out of the fourfold coincidence x-ray data only those events which were in coincidence with fourfold coincidence electron events falling in the electron window corresponding to the appropriate alphabetic label. The mass intervals associated with the x-ray spectra in this figure are those in which the x-rays appeared in their highest intensity. It is clearly seen from the K_α x-ray components in fig. 9 that electron peak A, B, C, D, and E arise from isotopes of Tc, Mo, Mo, Mo, and Ru respectively. Fig. 10 shows another example of the "x-ray window" analysis for the heavy fragment mass interval 139 - 141. In this figure, one sees that peak A contains contributions from an I and a Cs isotope and peak C contains contributions from a Cs and a Ba isotope. Peaks B and D are clearly identified with a Cs isotope and a Ba isotope respectively.

Determinations of the masses of the fragments responsible for the various electron peaks were made by plotting the intensities of x-rays derived from the "x-ray window sorts" as a function of mass. These plots for any given single electron peak uniquely establish the mass resolution and the first moment of the distribution identifies the true mass of the fission fragment. The average mass resolving functions for light and heavy fragments are shown in fig. 11. Each point on these curves represents an average of the points obtained in the analysis of eight individual light fragment electron peaks and ten individual heavy fragment electron peaks. The solid curves

drawn through the points are the result of least-squares Gaussian fits and the widths determined by these fits are 5.36 amu. (FWHM) for the light fragment resolving function and 6.56 amu. (FWHM) for the heavy fragment resolving function. The magnitude of the widths of these functions is determined by the dispersion introduced in neutron emission and by the inherent energy resolution of the fission fragment detectors. The difference in this width for heavy and light fragments is presumably a reflection of the fact that the detector resolution becomes worse with increasing particle mass and also may be indicative that the widths of the probability distributions for the emission of neutrons are substantially smaller for light fragments than for heavy fragments.

3.4 INTERPRETATION OF DATA

The results of the analysis of the data discussed in sections 3.1 and 3.3 are tabulated in table 1. Explanatory information pertaining to the various headings is as follows:

(1) Mass Number - - Determined from the centroid of a plot of electron peak intensities or coincident K x-ray intensities as a function of mass as discussed in section 3.3.

(2) Atomic Number - - Determined from the "x-ray window sorts" as discussed in section 3.3 for those cases in which the chemical symbol (in parentheses) follows the atomic number. For those cases in which only the atomic number is listed no determination was possible and the numbers listed are the atomic numbers of the most probable charge elements.

(3) K Line Energy - - These energies were determined from the least squares analysis of the triple coincidence electron spectra as

discussed in section 3.1. They have been corrected for momentum shift but not for binding energy shift (i.e. the same K line from stopped fission fragments would appear 0.9 kev higher than the listed energy).

(4) I_{rel} - - Under this heading are listed the intensities of the peaks as they appear in the 1 nsec electron spectra. These intensities are listed in units of 10^{-4} electrons/fission and the relative values are estimated to be accurate to ±10% for peaks above 50 kev and to ±20% for peaks below 50 kev.

(5) $t_{1/2}$ - - The listed transition half-lives were determined from the relative intensities of peaks appearing in the 1 nsec and 2 nsec electron spectra. These numbers are estimated to be accurate to better than ±20%. Transitions for which relative intensities appear but no half-lives are given decay with half-lives less than 0.5 nsec.

(6) I_{abs} - - The absolute intensities listed here were corrected for decay and are listed in units of 10^{-3} electrons/fission. The decay corrections were based upon the half-life determinations listed in the preceeding column. These intensities are estimated to be uncertain by ±25% for peaks above 50 kev and ±35% for peaks below 50 kev.

(7) γ-Ray Energy - - Gamma-ray energies not enclosed in parentheses were determined from the gamma-ray spectra of Bowman[2]) and of Cheifetz[13]). They are the energies of prominant gamma rays appearing in these spectra at positions predicted by the conversion electron energies and are estimated to be accurate to ±1 kev. Energies which are enclosed in parentheses are gamma-ray transition energies estimated

solely on the basis of the conversion electron energies and are given only for those cases in which clearly visible gamma rays could not be seen in the gamma-ray spectra.

(8) Confidence Level - - Three levels of confidence were used to grade the degree of certainty in the various assignments. Level A distinguishes those cases which were clearly enough resolved to allow relatively unambiguous determinations in mass, atomic number, and peak energy. For these cases the mass assignments are believed to be accurate to ±1 amu, the atomic number assignments are believed to be exact and the energy assignments are believed to be good to ±1 kev. Level B denotes cases in which interfering structure caused larger uncertainties in the mass and energy assignments (±2 amu and ±5 kev respectively). Level C was assigned to those cases in which interfering structure or low statistics gave rise to an uncertainty of ±1 in the atomic number assignments as well as to uncertainties in the mass and energy assignments. No confidence level was assigned to cases in which an atomic number determination was not possible.

(9) Observations - - Listed in this column are K to L electron intensity ratios (numbers in parentheses) for those cases where such a determination was possible. These ratios are to be taken as rough estimates since interfering structure in most cases prevented the accurate determination of L line intensities.

4. Discussion

A direct result of this study has been the observation of a large number of low energy transitions. These measurements have been particularly selective of low energy transitions, not only due to the energy dependence of conversion coefficients but also because of our focus on transitions having half lives of around one nanosecond. Nevertheless, these same transitions are the ones, in general, which predominate the low energy gamma-ray spectra obtained in studies having very little time selectivity. On the basis of such studies as, for example, those of Burde, Diamond and Stephens[14]), in which the only transitions observed in high intensity as a result of prompt deexcitation following heavy ion reactions are those belonging to rotational or quasi-rotational cascades in the ground state band, one might expect that the majority of the transitions we observe are likewise linked with cascades from levels near the ground state. Clearly a necessary condition for the existence of high intensity transitions is that there be a high probability for populating the same levels or sequence of levels each time a particular fission product is formed. It seems extremely unlikely that such conditions exist at high excitation energies and therefore it is presumed that the majority of the observed transitions arise from levels located near the ground state.

In considering the probable origin of these low energy transitions, even-even nuclei, for the most part, must be eliminated from consideration as major contributors since only in regions of permanent deformation do level spacings near the ground state in even-even nuclei become smaller than several hundred keV. In this connection, we refer to fig. 12 where the

x-ray spectrum (b) arising from fission fragments within the time interval of 0 to 100 nanoseconds after fission is compared with the x-ray spectrum (a) arising from fission fragments within the time interval of approximately 0.1 to 1.9 nanoseconds after fission. The latter, spectrum (a), was obtained from the four-fold coincidence data and represents the spectrum of x-rays coincident with complementary fragment pairs and conversion electrons. (X-rays contributing to this spectrum are emitted as a direct result of the internal conversion of the transitions observed in the electron spectra.) A surprising feature in spectrum (a) is the extremely small relative contribution of x-rays from products above Pr (36 keV) in comparison with spectrum (b). Contributions to the x-ray spectrum from even-even nuclei were expected to be especially important in this region since this is the beginning of the rare earth region of stable deformation characterized by low 2+ to 0+ rotational transition energies. A survey of the known systematics of some even-even nuclides in this deformed region is summarized in table 2. Here it is seen that the first 2+ state in Nd and Sm isotopes having 90 or more neutrons lies below 150 keV and even reaches as low as 75 keV out at the 96 neutron nucleus ^{160}Gd. The half lives of these states range from one to three nanoseconds. Since substantial yields of Nd and Sm isotopes are formed in the fission of ^{252}Cf (estimated combined yields are 2.3% for $^{150\ 152\ 154}$Nd and 0.6% for $^{154\ 156\ 158}$Sm)[15]), we conclude, on the basis of fig. 12, that even-even nuclei make relatively little contribution to the heavy fragment conversion electron spectra and therefore that the majority of the low energy transitions we observe belong to odd-mass or odd-odd nuclei. Moreover, it can be stated, from an examination of the highest intensity x-ray components appearing in spectrum (a) of fig. 12, that these low energy transitions are associated almost exclusively with isotopes of Zr, Mo, Tc, Ru, I, Cs, Ba, La, Ce and Pr.

Another general observation pertaining to the origin of the low energy transitions seen in our studies can be made in reference to fig. 13 in which is shown a contour plot of the number of K x-rays emitted per fission in the time interval of 0 to 100 nanoseconds. This figure was constructed from the three-fold x-ray coincidence data by analyzing each of the mass sorted x-ray spectra using a computerized least-squares peak fitting procedure described in ref.[16]). In this way, the intensities of x-rays associated with every mass interval were determined for each element. Relative to the present discussion, fig. 13 is interesting because it shows the occurrence of several intense peaks which in every case center at an odd-odd nucleus. High intensity peaks occur in the light fragment region at $^{108}_{43}TC_{65}$ and in the heavy fragment region at $^{136}_{53}I_{83}$, $^{140}_{55}Cs_{85}$, and $^{146}_{57}La_{89}$. Apparently these particular nuclei all have one or more especially intense transitions which are highly converted. This evidence further suggests that odd-odd nuclei, in general, are substantial contributors to the spectra we observe.

Referring back to table 1, it may be seen that the above conclusions are well substantiated. Most of the lines in this table are assigned to odd-mass or odd-odd nuclei. The aforementioned x-ray intensity peaks (fig. 13) are accounted for by high intensity transitions occurring at 69 keV in ^{108}Tc, 59 keV in ^{136}I, 78 keV in ^{140}Cs, and 64 keV in ^{146}La. A number of lines have also been assigned to even-even nuclei in the light fragment region. Transitions occurring in the region near mass 110 are of special interest as a consequence of the predictions of Johansson[17]) and of the Myers and Swiatecki mass formula[18]) which suggest this as a possible region of stable deformation. Based on previous conversion electron measurements, Watson[2]) picked two lines estimated to arise from a 98 keV and a 238 keV gamma-ray transition as candidates for possible

2+ to 0+ and 4+ to 2+ transitions in ^{110}Ru. Based on analogy with these assignments, Zicha et al.[19]) have deduced from their results similar decay schemes for ^{106}Ru and ^{108}Ru. The present measurements, however, have established that the 98 keV gamma ray belongs instead to a Tc isotope, most probably ^{108}Tc, but also substantiate Watson's original assignment of the 238 keV transition to ^{110}Ru (see peak E in fig. 9). In light of the present results and because of the unreasonably large quadrupole moment and deformation (Q_0 = 7.3 b, β = 0.55) predicted for ^{106}Ru by their studies, the conclusions of Zicha et al. appear questionable.

In the present study, the energy of the converison electron line was measured to be 218 keV corresponding to a gamma-ray transition of 241 keV. It appears to be of E2 character based on the observed K to L conversion electron ratio. In a study of fission product deexcitation following beta decay, Wilhelmy[20]), reports observing a strong transition at 240.67 ± 0.11 keV associated with a half life of 0.825 ± 0.039 seconds which he proposes as a transition in ^{110}Ru populated by the beta decay of ^{110}Tc. Recently, Cheifetz[13]) has studied the angular correlation of prompt gamma-rays emitted from ^{252}Cf fission fragments using a technique in which the fragments are stopped in a thick backing. By eliminating the Doppler shift problem, he was able to obtain accurate gamma-ray energies. He identified a transition at 241.3 keV which has an anisotropy consistent with that of an aligned E2 transition and an intensity corresponding to ~100% of the calculated yield of ^{110}Ru. On the basis of these results, we propose the 241 keV transition as the first 2+ to 0+ transition in ^{110}Ru.

With regard to the possible deformed character of ^{110}Ru, it is instructive to estimate the expected energy of the first 2+ state based on the assumption of rotational behavior. Using the Myers and Swiatecki mass formula[21]), we

estimate a deformation parameter for ^{110}Ru of $\beta = 0.23$. Assuming the moment of inertia ratio I/Irig to be the same as for deformed rare-earth nuclei, we obtained from the graph of I/Irig versus β given by Diamond, Stephens and Swiatecki[22]) the value of I/Irig = 0.28. Using this, the rotational constant is calculated to be $\hbar^2/2I = 38$ keV, which gives for the estimated 2+ state energy

$$E_{2+} \cong \frac{\hbar^2}{2I}(2)(2+1) = 228 \text{ keV}.$$

Further insight into the possibility that ^{110}Ru is a deformed nucleus may be gained by comparing the systematics of the first excited levels in the heaviest Ru isotopes with those observed in the rare earth region. Fig. 14 is a graph of the energies of the first 2+ states in even-even Ru isotopes. The numbers in parentheses are the energy ratios $E_{4\to2}/E_{2\to0}$. The values shown for ^{106}Ru and ^{108}Ru were taken from the data of Von Baeckmann and Feuerstein[23]) and from Wilhelmy and are to be considered tentative. It is seen that the 241 keV gamma-ray which we propose as the first 2+ to 0+ transition in ^{110}Ru fits the systematics quite well. Also shown by the dotted line are the values of $(E_{2+})_{crit} = 13\hbar^2/I_{rig}$. This is the energy criterion suggested by Alder et al.[24]) according to which nuclei having $E_{2+} > (E_{2+})_{crit}$ may be assumed to be spherical and those having $E_{2+} < (E_{2+})_{crit}$ may be assumed to be deformed. In fig. 15 we present a similar graph showing the systematics of the first excited states in even-even Gd isotopes. It is observed in this figure, that the transition from spherical to deformed behavior is characterized by a rapid drop in the energy of the first 2+ level accompanied by an increase in the $E_{4\to2}/E_{2\to0}$ energy ratio. As the energy ratio approaches 2.33, the value for a rigid rotor, the energy of the first 2+ state no longer changes greatly from isotope to isotope and eventually remains nearly constant. The

qualitative similarities between fig. 14 and fig. 15 strongly suggest that ^{110}Ru does indeed belong to a new region of stable deformation.

Among the lines assigned to heavy fission fragments in table 1, one in particular appears to be a good candidate for an even-even 2+ to 0+ transition from the standpoint of energy; namely the 158 keV gamma transition assigned to ^{148}Ce. Wilhelmy has detected a strong transition at 158.45 ± 0.08 keV having a half life of 1.29 ± 0.08 seconds and as a consequence of the present observations has assigned it to the beta decay of ^{148}La feeding the first 2+ level of ^{148}Ce. In fig. 16 we present a graph showing the first 2+ level systematics of even-even Ce isotopes. The energy of the 2+ state in ^{142}Ce (E_{2+} = 641.6 keV) was taken from the results of Alvager et al.[25]).

Another strong transition of 199 keV is proposed as the first 2+ to 0+ transition in ^{144}Ba. It appears to have the required E2 multipolarity as determined from the ratio of K to L electron intensities. This line has also been seen by Cheifetz, who finds it exhibits an anisotropy of the kind expected for an aligned E2 transition and by Wilhelmy, who obtained an accurate energy determination of 199.31 ± 0.17 keV and a measured beta decay half life of 1.01 ± 0.05 seconds. The systematics of even-even Ba isotopes are shown in fig. 17. The energies of the first 2+ states in ^{140}Ba and ^{142}Ba (E_{2+}= 602 and 361 keV respectively) were taken from the results of Alvager et al.[25]). From this figure, it is evident that the first 2+ level decreases rapidly in energy in either direction as one proceeds away from the large discontinuity at the 82 neutron configuration. It appears that ^{144}Ba (having 88 neutrons) is on the borderline between deformed and transitional nuclei.

The known transitions of ^{153}Eu provide an insight into the character of typical odd-mass transitions in the heavy mass region. The ground state has spin and parity 5/2+ while the first two excited levels are a 7/2+, 83 keV state and a 9/2+, 191 keV state. Deexcitation proceeds via a two transition

M1-E2 cascade and a crossover transition from the 9/2+ level to the ground state in relative amounts of 26% and 74% respectively. The 9/2+ level has a half life of 0.24 nsec and the 7/2+ level has a 0.7 nsec half life. Strong cross-over transitions are known for a number of other odd-mass nuclides in this region, for example the cross-over transition (64% relative intensity) having an energy of 256 keV and a half-life of 0.9 nsec in ^{151}Pm. In searching for lines having these characteristics, a number of possible cross-over transitions were found. In particular, the gamma ray lines assigned to masses 144, 146, and 149 at energies of 283, 296, and 245 keV respectively are of about the right energies for cross-over transitions. Very little information could be obtained for these particular transitions, however, because their intensities were quite low - nor could any substantial evidence be found of the appearance of cascade transitions whose energies would sum to any of the proposed cross-over energies. Alvager et al.[25]) in their study of mass-separated xenon fission products have observed strong transitions of equal intensities at 79.4 keV and 117.5 keV which they have assigned to a cascade from the second excited state to the ground state in ^{140}Cs. We see a very strong transition at 78 keV associated with ^{140}Cs and another strong transition of about the same intensity at 118 keV which belongs to a Cs isotope in the vicinity of mass 140 (a good mass determination for this line was not possible because of interference from another electron line). We believe these two transitions are the same as those reported by Alvager et al.

5. Conclusion

The results of these experiments have shown that the study of the conversion electrons emitted in fission is an effective way to obtain detailed information on the low-energy transitions in primary fission fragments. The experimental techniques developed in these investigations have enabled a selectivity which is unattaninable in the study of the gamma-rays, both with

respect to separating radiation emitted from different members of coincident fragment pairs and with respect to measuring the spectra associated with definite and well-defined time intervals after fission. A serious restriction, however, is imposed upon the energy resolution obtainable in such experiments as a consequence of the motion of the fission fragments. The major limitation in these studies with regard to constructing detailed decay schemes has been the relatively large uncertainty in the mass assignments. Should future advances evolve more accurate techniques which can be utilized in high detection geometry configurations for measuring fission fragment masses, the methods developed here may be of considerable use in enabling detailed nuclear spectroscopic investigations to be carried out on the ultra neutron excess nuclei produced by fission.

Acknowledgments

It is a pleasure to thank Dr. E. Cheifetz for many helpful discussions concerning this work and for the use of his unpublished data. We also wish to thank Dr. Robert Latimer and Mr. Raymond Gatti for help in preparing the ^{252}Cf source and Mrs. Joan Phillips, Mr. James Sjurseth, and Mr. Robert Howard for assistance in analyzing the data.

Appendix

FISSION FRAGMENT MASS COMPUTATION

Several problems complicate the conversion of fission fragment kinetic energies as measured by semiconductor detectors into fission fragment masses. First of all, it has been found that for heavy ions the output pulse heights of semiconductor detectors are not strictly linear functions of energy because of the existence of a pulse height defect[26,27]). Secondly, the measured energies are those of the post-neutron-emission fragments since neutron emission occurs in a time less than 10^{-14} sec after scission. Therefore, the exact conversion of these energies to masses requires a knowledge of the numbers of neutrons which have been emitted.

In the present experiments, the energy to mass conversion was carried out by means of an iterative process which incorporated a mass dependent energy calibration, proposed by Schmitt et.al.[28]) and neutron corrections based on the measurements of Bowman et.al.[29]). The process was initiated for any given pair of coincident fission fragment pulse heights, designated as X_1 and X_2, by first computing their approximate energies from a linear calibration equation established from the known energies of the first moments between the 3/4 points of the heavy and light fragment peaks. The first moments, P_L and P_H, were determined from the double-coincidence stabilization fission fragment distributions and set equal to energy values of 103.77 Mev and 79.37 Mev respectively[28]). Thus

$$E \cong MX + b \qquad (1)$$

where

$$M = \frac{24.40}{P_L - P_H} \quad .$$

Conservation of momentum requires that

$$\frac{E_{1p}}{E_{2p}} = \frac{M_{2p}}{M_{1p}} \quad . \qquad (2)$$

(The subscript p denotes pre-neutron-emission quantities.)

One furthur condition is

$$M_{1p} + M_{2p} = 252 \quad . \qquad (3)$$

Using E_1 and E_2 (post-neutron-emission kinetic energies) as estimates for E_{1p} and E_{2p}, approximate pre-neutron-emission masses are then calculated from the expressions

$$M_{1p} \cong \frac{252}{(1+\frac{E_1}{E_2})} \qquad (4)$$

$$M_{2p} = 252 - M_{1p} \quad .$$

Also, the total kinetic energy is estimated by

$$E_T = E_{1p} + E_{2p} \cong E_1 + E_2 \; . \qquad (5)$$

The approximated values of M_{1p} and M_{2p} are next corrected for neutron emission using Bowman et.al.'s measurements of the average number of neutrons emitted as a function of E_T and the average number of neutrons emitted as a function of mass. A fit of the experimental data by Takekoshi and Thompson[30]) yielded the following empirical dependence of the average total number of neutrons, ν_T, emitted in a ^{252}Cf fission event:

$$\nu_T = A(m)e^{-B(m)(E_T - 150.0)} \; . \qquad (6)$$

Values of the parameters A(m) and B(m) are given in ref.[30]). Using the

calculated ν_T and taking the ratio of the number of light fragment neutrons to the number of heavy fragment neutrons from ref.[29]), first approximation post-neutron-emission masses are computed

$$M_1 = M_{1p} - \nu_1$$

$$M_2 = M_{2p} - \nu_2$$

At this point, "mass corrected" energy values are calculated from the original pulse heights, using the approximate post-neutron-emission masses, according to the mass dependent calibration equation of Schmitt et.al.

$$E' = (24.0203 + 0.03574M)\frac{X}{P_L - P_H} - (24.0203 + 0.03574M)\frac{P_L}{P_L - P_H} + 0.1370M + 89.6083 \quad . \qquad (7)$$

Then, since neutron emission does not significantly alter the fragment velocities,

$$E'_{1p} = E'_1 \left(\frac{M_{1p}}{M_{1p} - \nu_1}\right) \qquad (8)$$

and similarly for E'_{2p} .

The iterative process is entered into by returning to eq. (5) using the energy values obtained from eq. (8) and recalculating the post-neutron-emission masses. This procedure is repeated until the difference in the mass values resulting from two consecutive iterations is less than 0.05%. On the average, not more than four iterations are required for convergence.

Since the fission fragment masses are derived from measured fragment kinetic energies, any dispersion introduced into the energy measurements

will also be reflected in the calculated mass distributions. It has been pointed out by Terrell[31]) that, besides arising from instrumental effects and intrinsic detector resolution, a great deal of dispersion in the energy measurements arises as a result of the varying directions, energies, and numbers of emitted neutrons. The combination of these effects is what gives rise to the mass dispersion functions shown in fig. 11. In comparing an experimentally measured mass distribution with the "true" mass distribution, the former is generally considerably broader, especially in the valley and light-and heavy-peak tail regions as a result of the experimental mass dispersion. The usual way of removing this dispersion is by the method of Terrell in which a symmetric distribution function having a negative second central moment equal to the variance of the measured mass resolution function is folded into the experimental mass distribution. This procedure has the effect of reducing the variance of the mass distribution by an amount equal to the variance of the experimental resolution function.

A comparison of the mass distribution for ^{252}Cf calculated by our iterative procedure (uncorrected for dispersion) with the radiochemical mass distribution determined by Nervik[32]) is shown in fig. 18. As can be seen, our "uncorrected" distribution gives a surprisingly good representation of the true mass distribution. Apparently the method we use to calculate the measured mass distribution has the same resolving effect as Terrell's procedure. On the basis of fig. 17, then, the usual dispersion correction was assumed to be unnecessary in the present experiments.

TABLE 1

Interpretation of Data[a]

Mass Number	Atomic Number	K Line Energy (keV)	I_{rel}	$t_{1/2}$ (nsec.)	I_{abs}	γ-Ray Energy (keV)	Confidence Level	Observations
98	40(Zr)	194	1.2			213	B	
101	40(Zr)	80	13			99	C	
102	40(Zr)	134	4.9	1.7	1.6	153	B	
	40(Zr)	189	2.5			(208)	A	
106	42(Mo)	74	27	1.1	6.2	95	A	K to L ratio (4.8) consistent with E2
	42(mo)	130				(151)	B	
	42(Mo)	151				172	A	
	42(Mo)	171	11	1.2	8.1	192	A	
107	43(Tc)	44	25	1.0	6.0	(66)	C	
108	43(Tc)	47	47	1.0	11	69	A	
	43(Tc)	76	12	0.9	2.7	98	B	
109	43(Tc)	101	4.3			123	A	
110	44(Ru)	49	18	2.2	7.5	72	B	
	44(Ru)	127				150	C	
	44(Ru)	218	4.7	<0.5		241	A	K to L ratio (4.0) consistent with E2

TABLE 1 (Continued)

Mass Number	Atomic Number	K Line Energy (keV)	I_{rel}	$t_{1/2}$ (nsec.)	I_{abs}	γ-Ray Energy (keV)	Confidence Level	Observations
113	45(Rh)	38	8.7			(62)	C	
116	46(Rh)	24	4.3	0.6	0.82	49	A	K to L ratio (2.4) consistent with E2
136	53(I)	25	10			59	B	
	53(I)	54	2.5	0.4	0.56	(88)	B	
139	54	251	0.38			283		
140	55(Cs)	24				(61)	B	
	55(Cs)	41	44	1.0	11	78	A	
	55(Cs)	81	18	2.6	8.8	118	B	K to L ratio (5.3) consistent with M1
143	55(Cs)	75				112	C	
144	56(Ba)	75	30	1.2	9.4	113	B	
	56(Ba)	145				183	A	
	56(Ba)	161	9.4	1.0	2.5	199	A	K to L ratio (4.1) consistent with E2
	56	245	0.27			283		
145	57(La)	60	15	1.7	7.3	100	C	
146	57(La)	24	39	0.6	9.4	64	A	K to L ratio (2.5) consistent with E2

TABLE 1 (Continued)

Mass Number	Atomic Number	K Line Energy (keV)	I_{rel}	$t_{1/2}$ (nsec.)	I_{abs}	γ-Ray Energy (keV)	Confidence Level	Observations
	57(La)	91	7.2	2.7	2.0	131	A	
	57	256	0.17			296		
148	58(Ce)	117	11	1.3	3.4	158	A	K to L ratio (3.7) consistent with E2
149	59(Pr)	100	8.4	1.8	3.2	143	A	K to L ratio (3.6) consistent with E2
	58	204	0.36			(245)		
150	59(Pr)	23				66	C	
	59(Pr)	31	30	1.4	9.9	74	A	
152	58(Ce)	122				163	B	
156	62(Sm)	24	4.8	2.9	2.6	72	C	K to L ratio (1.7) consistent with E2
	62	43	2.7	1.9	1.1	91		
158	62	66	7.9	1.9	3.2	(114)		
	62	70				(118)		

(a) See section 3.4 for explanatory remarks.

TABLE 2

Systematics of even-even first 2+ states in rare earth region

Nuclide	First 2+ Energy (keV)	$t_{1/2}$ (nsec)
$^{142}_{58}Ce_{84}$	640	0.006
$^{144}_{60}Nd_{84}$	696	0.008
$^{146}_{60}Nd_{86}$	453	0.06
$^{148}_{62}Sm_{88}$	334	0.05
$^{148}_{60}Nd_{88}$	300	0.2
$^{150}_{62}Sm_{88}$	334	0.05
$^{152}_{64}Gd_{88}$	344	0.05
$^{150}_{60}Nd_{90}$	132	1.6
$^{152}_{62}Sm_{90}$	122	1.4
$^{154}_{64}Gd_{90}$	123	1.2
$^{154}_{62}Sm_{92}$	82	3.0
$^{156}_{64}Gd_{92}$	89	2.2
$^{160}_{64}Gd_{96}$	75	2.5

FIGURE CAPTIONS

Fig. 1. Schematic diagram of experimental arrangement.

Fig. 2. Energy spectra of internal conversion electrons emitted in coincidence with fission fragments of all masses at the approximate average times of (a) 0.4 nsec after fission, (b) 1 nsec after fission, and (c) 2 nsec after fission.

Fig. 3. Mass sorted energy spectra of internal conversion electrons emitted in coincidence with heavy fission fragments belonging to three different intervals of mass and taken at the approximate average time of 1 nsec after fission.

Fig. 4. Mass sorted energy spectra of internal conversion electrons emitted in coincidence with light fission fragments belonging to two different intervals of mass and taken at the approximate average time of 1 nsec after fission.

Fig. 5. A comparison of two mass sorted electron spectra for a heavy fragment mass interval; one taken at an approximate average time of 1 nsec after fission and the other taken at an approximate average time of 2 nsec after fission.

Fig. 6. Mass sorted gamma-ray spectra in coincidence with complimentary heavy and light fragment pairs. A number of the peaks are labeled alphabetically to identify them with the associated electron peaks in figs. 3 and 4.

Fig. 7. A Mass sorted electron spectrum which has been analyzed with a computerized Gaussian fitting procedure.

Fig. 8. The yield of low energy internal conversion electrons as a function of fission fragment mass over the two approximate time intervals of 0.1 to 1.9 nsec after fission and 1.1 to 2.9 nsec after fission.

Fig. 9. An electron spectrum for the light fragment mass interval 107-109 and the K x-ray spectra resulting from "x-ray window sorts" on the alphabetically labelled electron peaks. The x-ray spectra shown are for the mass intervals in which the x-rays appeared in their highest intensities.

Fig. 10. An electron spectrum for the heavy fragment mass interval 139-141 and the K x-ray spectra resulting from "x-ray window sorts" on the alphabetically labelled electron peaks. The x-ray spectra shown are for the mass intervals in which the x-rays appeared in their highest intensities.

Fig. 11. The average mass resolving functions for light and heavy fragments.

Fig. 12. The spectra of K x-rays (a) arising from fission fragments within the approximate time interval of 0.1 to 1.9 nsec after fission and (b) arising from fission fragments within the approimate time interval of 0 to 100 nsec after fission.

Fig. 13. A contour plot of the intensity of x-rays arising from fission fragments within the approximate time interval of 0 to 100 nsec after fission as a function of atomic number and neutron number.

Fig. 14. The systematic variation of the first excited states in even-even Ru isotopes. Numbers in parentheses are the ratios of the energies of the second excited states to the energies of the first excited states and the dashed line is a plot of (E_{2+})crit.

Fig. 15. The systematic variation of the first excited states in even-even Gd isotopes. Numbers in parentheses are the ratios of the energies of the second excited states to the energies of the first excited states and the dashed line is a plot of (E_{2+})crit.

Fig. 16. The systematic variation of the first excited states in even-even Ce isotopes. The dashed line is a plot of (E_{2+})crit.

Fig. 17. The systematic variation of the first excited states in even-even Ba isotopes. The dashed line isa plot of (E_{2+})crit.

Fig. 18. A comparison of the ^{252}Cf fission fragment distribution obtained from the analysis of a double coincidence semiconductor pulse-height spectrum with the radiochemical results of Nervik[32]).

REFERENCES

1) H. R. Bowman, S. G. Thompson and J. O. Rasmussen, Phys. Rev. Lett. 12 (1964) 195

2) R. L. Watson, (Ph.D. Thesis), University of California Lawrence Radiation Laboratory Report No. UCRL-16798, 1966 (unpublished)

3) H. R. Bowman, University of California Lawrence Radiation Laboratory, Berkeley, California, unpublished data

4) R. L. Watson, J. O. Rasmussen, H. R. Bowman, and S. G. Thompson, Rev. Sci. Instr. 38 (1967) 905

5) Richard C. Jared and George W. Kilian, University of California, Lawrence Radiation Laboratory Report No. UCRL-17528, 1967 (unpublished)

6) M. Nakamura and R. LaPierre, Nucl. Instr and Meth. 32 (1965) 277

7) R. L. Watson, H. R. Bowman, S. G. Thompson and J. O. Rasmussen, University of California, Lawrence Radiation Laboratory Report No. UCRL-17289, 1967 (unpublished)

8) R. L. Watson and J. O. Rasmussen, J. Chem. Phys. 47 (1967) 778

9) R. A. Atneosen, T. D. Thomas, W. M. Gibson, and M. L. Perlman, Phys. Rev. 148 (1966) 1206

10) L. E. Glendenin and J. P. Unik, Phys. Rev. 140 (1965) B 1301

11) S. S. Kapoor, H. R. Bowman and S. G. Thompson, Phys. Rev. 140 (1965) B 1310

12) R. L. Watson, R. C. Jared and S. G. Thompson, to be submitted to Phys. Rev.

13) E. Cheifetz, University of California, Lawrence Radiation Laboratory, Berkeley, California, unpublished data

14) J. Burde, R. M. Diamond and F. S. Stephens, Nucl. Phys. A92 (1967) 306

15) R. L. Watson and J. B. Wilhelmy, University of California, Lawrence Radiation Laboratory Report No. UCRL-18632, 1969 (unpublished)

16) R. L. Watson, H. R. Bowman and S. G. Thompson, Phys. Rev. 162 (1967) 1169

17) S. A. E. Johansson, Nucl. Phys. 60 (1964) 378

18) W. D. Myers and W. J. Swiatecki, Nuc. Phys. 81 (1966) 1

19) G. Zicha, K. E. G. Lobner, P. Maier-Komor, J. Maul and P. Kienle, paper presented at the International Conference on Properties of Nuclear States, Montreal (August, 1969)

20) J. B. Wilhelmy (Ph.D. Thesis) University of California, Lawrence Radiation Laboratory Report No. UCRL-18978, 1969 (unpublished)

21) W. D. Myers and W. J. Swiatecki, University of California, Lawrence Radiation Laboratory Report No. UCRL-11980, 1965 (unpublished)

22) R. M. Diamond, F. S. Stephens and W. J. Swiatecki, Phys. Lett. 11 (1964) 315

23) A. Von Baeckmann and H. Feuerstein, Radiochimicacta 5 (1966) 235

24) K. Alder, A. Bohr, T. Huus, B. Mottelson and A. Winther, Rev. Mod. Phys. 28 (1956) 432

25) T. Alvager, R. A. Naumann, R. F. Petry, G. Sidenius, and T. Darrah Thomas, Phys. Rev. 167 (1967) 1105

26) C. W. Williams, W. E. Kiker, and H. W. Schmitt, Rev. Sci. Instr. 35 (1964) 1116

27) H. W. Schmitt, W. M. Gibson, J. H. Neiler, F. J. Walter and T. D. Thomas, Proceedings of the IAEA Conference on the Physics and Chemistry of Fission, Salzburg, Austria, 1965 (International Atomic Energy Agency, Vienna, 1965) Vol. I, p. 385

28) H. W. Schmitt, W. E. Kiker and C. W. Williams, Phys. Rev. 137 (1965) B837

29) H. R. Bowman, J. C. D. Milton, S. G. Thompson and W. J. Swiatecki, Phys. Rev. 126 (1962) 2120; 129 (1963) 2133

30) E. Takekoshi and S. G. Thompson, University of California, Lawrence Radiation Laboratory Report No. UCRL-17299, 1967 (1966 annual report)

31) J. Terrell, Phys. Rev. 127 (1962) 880

32) W. E. Nervik, Phys. Rev. 119 (1960) 1685

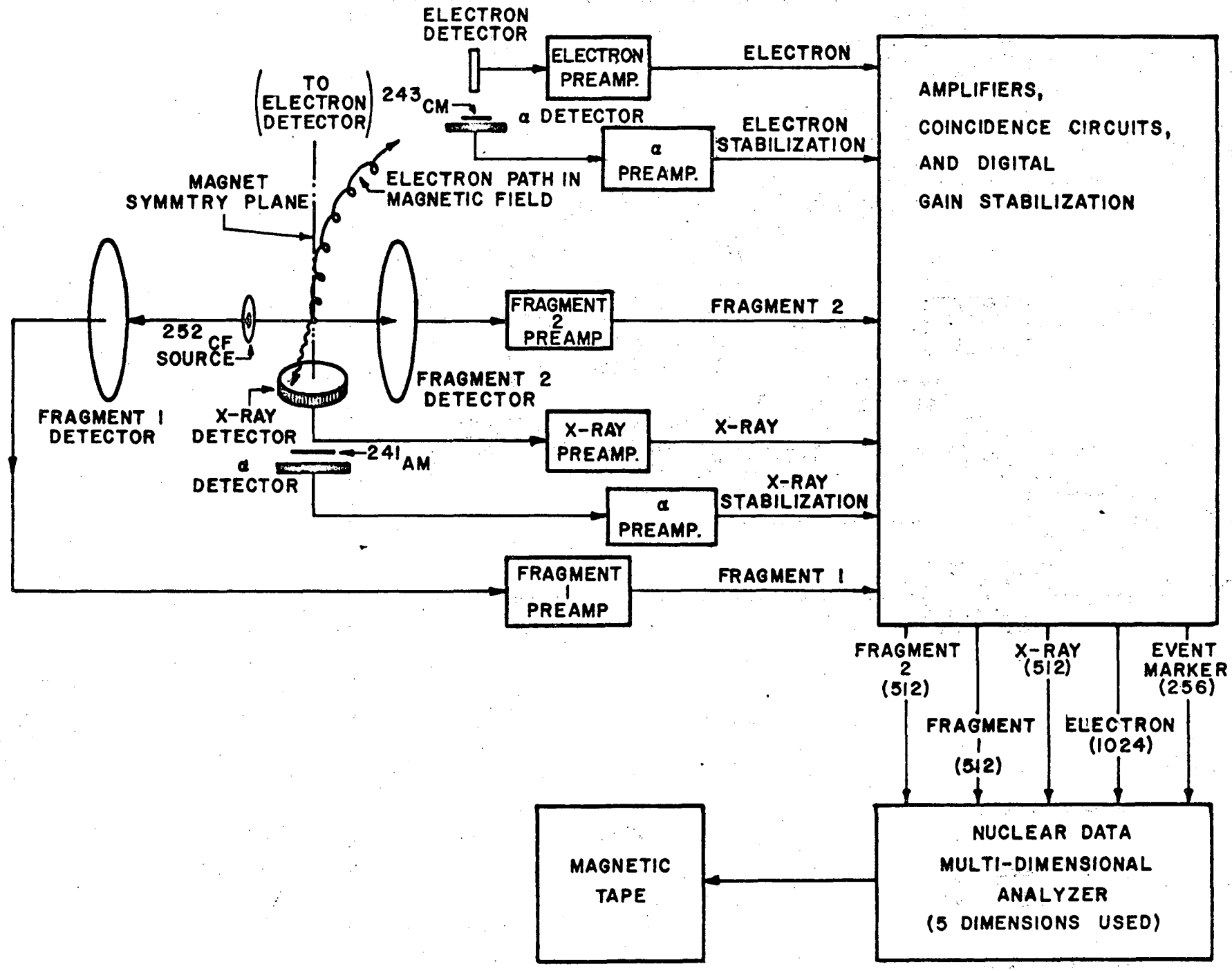
ELECTRON DETECTOR
ELECTRON PREAMP.
ELECTRON
AMPLIFIERS, COINCIDENCE CIRCUITS, AND DIGITAL GAIN STABILIZATION
TO ELECTRON DETECTOR
243 CM
α DETECTOR
α PREAMP.
ELECTRON STABILIZATION
MAGNET SYMMTRY PLANE
ELECTRON PATH IN MAGNETIC FIELD
FRAGMENT 2 PREAMP
FRAGMENT 2
252 CF SOURCE
FRAGMENT 2 DETECTOR
FRAGMENT 1 DETECTOR
X-RAY DETECTOR
X-RAY PREAMP.
X-RAY
241 AM
α DETECTOR
α PREAMP.
X-RAY STABILIZATION
FRAGMENT 1 PREAMP
FRAGMENT 1
FRAGMENT 2 (512)
X-RAY (512)
EVENT MARKER (256)
FRAGMENT 1 (512)
ELECTRON (1024)
MAGNETIC TAPE
NUCLEAR DATA MULTI-DIMENSIONAL ANALYZER (5 DIMENSIONS USED)

Fig. 1

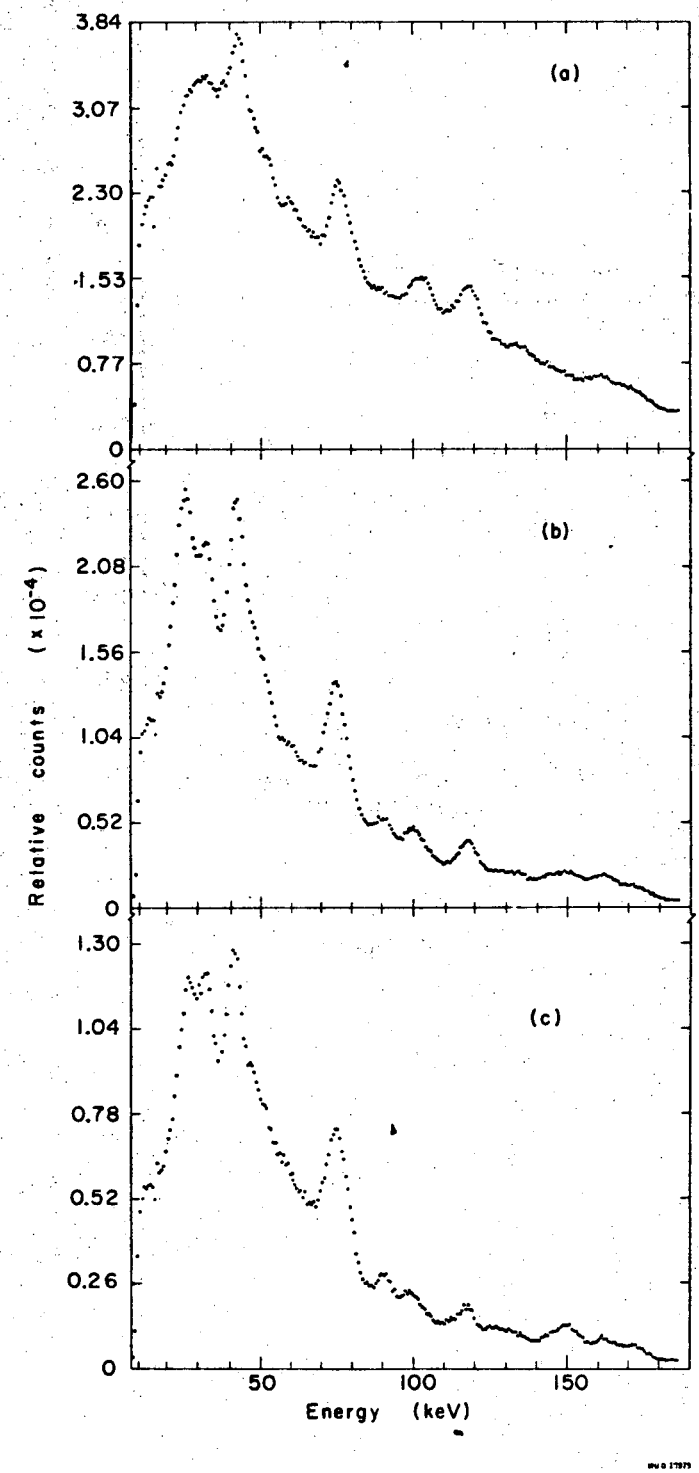
3.84
3.07
2.30
1.53
0.77
0
(a)
2.60
2.08
1.56
1.04
0.52
0
(b)
1.30
1.04
0.78
0.52
0.26
0
(c)
Relative counts (x 10^-4)
50
100
150
Energy (keV)

Fig. 2

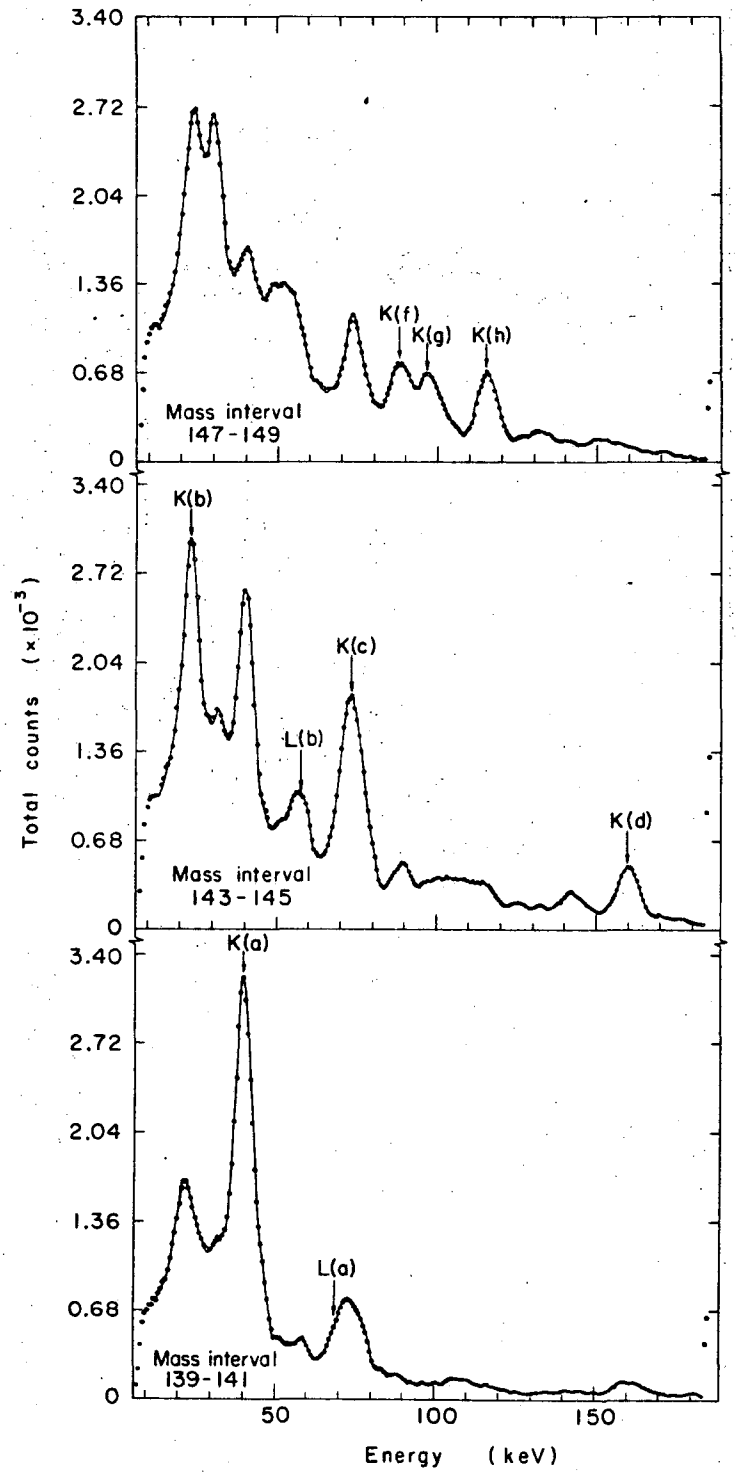
3.40
2.72
2.04
1.36
0.68
0
K(f)
K(g)
K(h)
Mass interval
147-149
K(b)
K(c)
L(b)
K(d)
Mass interval
143-145
K(a)
L(a)
Mass interval
139-141
Total counts (×10⁻³)
50
100
150
Energy (keV)

Fig. 3

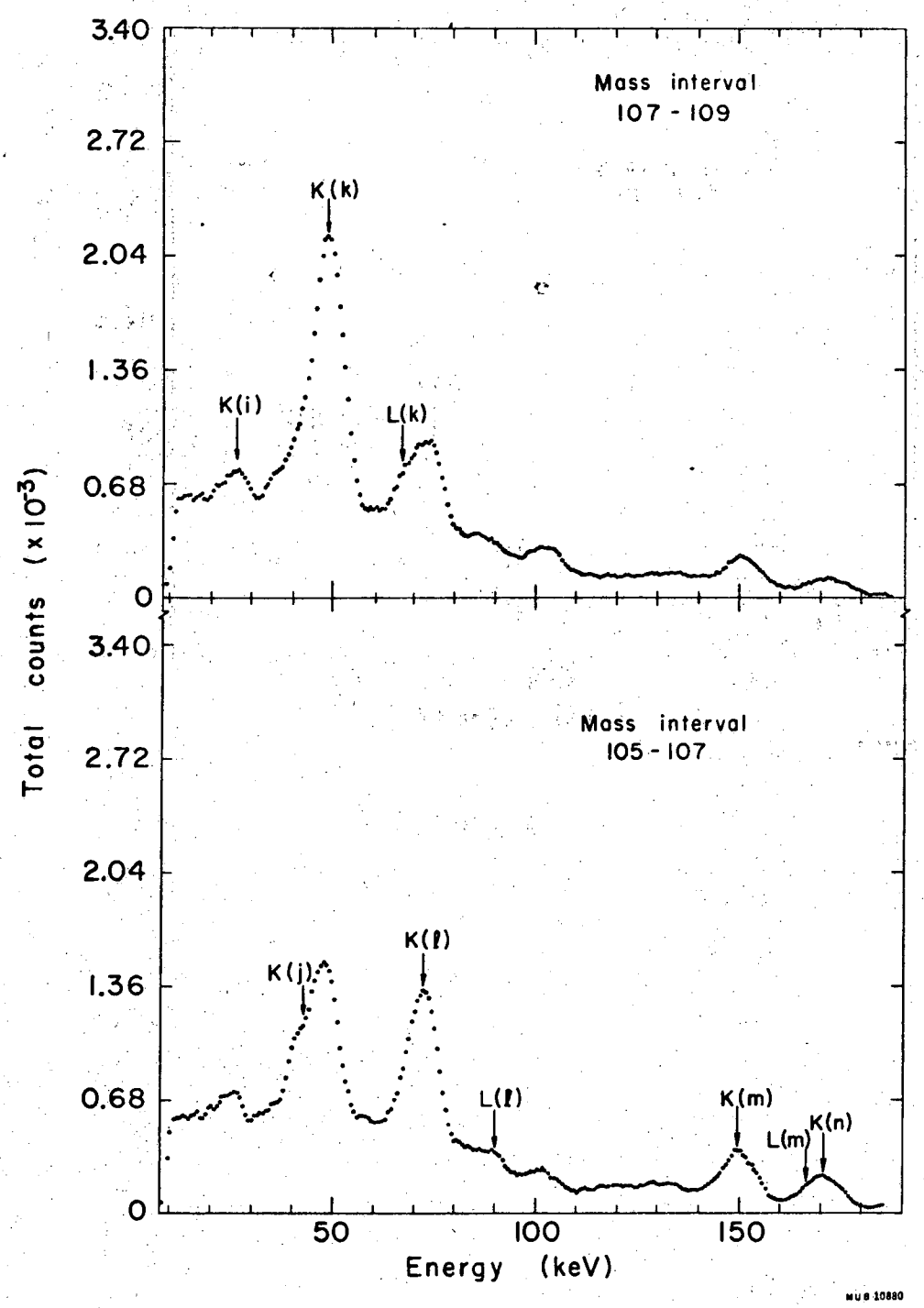
Mass interval
107 - 109
K(k)
K(i)
L(k)
Mass interval
105 - 107
K(j)
K(ℓ)
L(ℓ)
K(m)
L(m)
K(n)
3.40
2.72
2.04
1.36
0.68
0
Total counts (x 10^-3)
50
100
150
Energy (keV)
MU 8 10880

Fig. 4

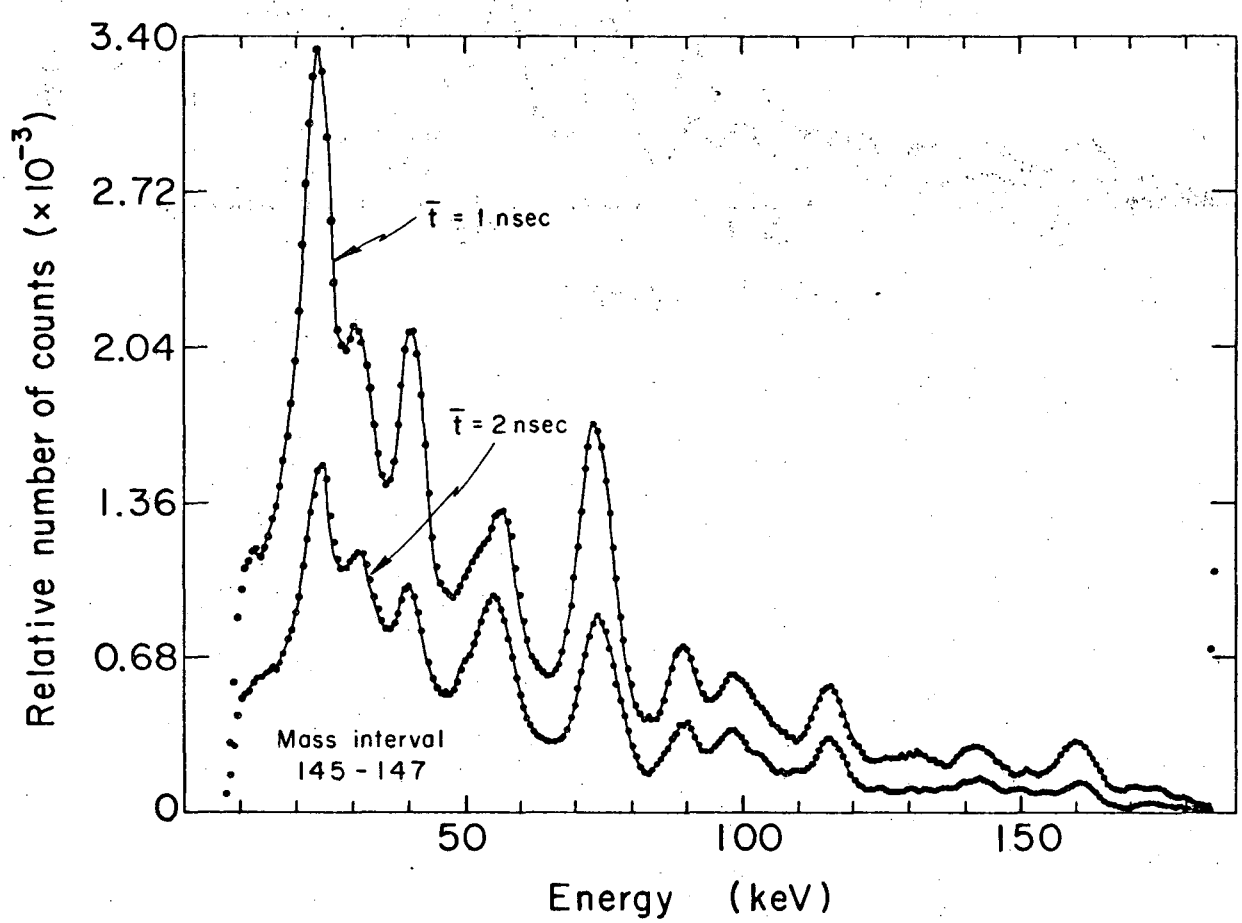

MUB-9908

Fig. 5

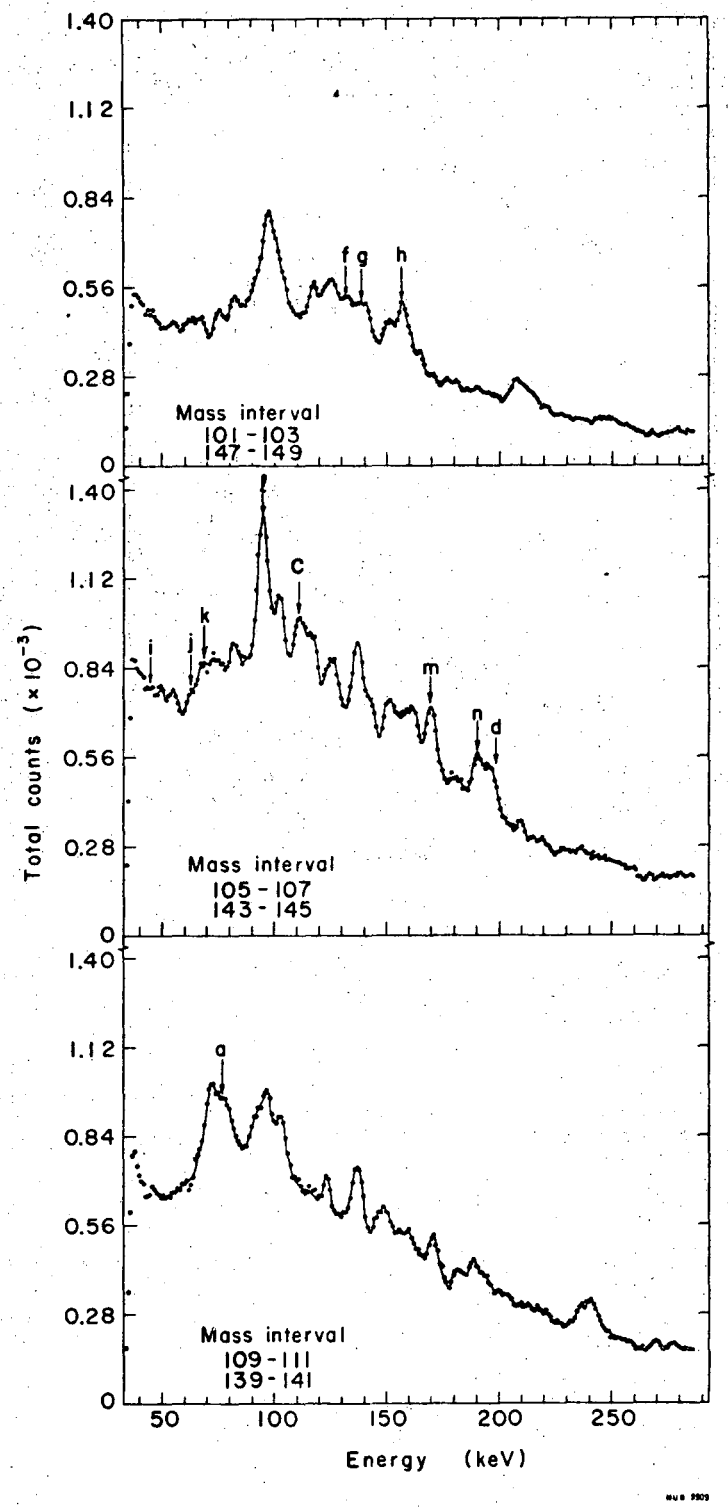
1.40
1.12
0.84
0.56
0.28
0
f g h
Mass interval
101 - 103
147 - 149
c
k
j
i
m
n
d
Mass interval
105 - 107
143 - 145
a
Mass interval
109 - 111
139 - 141
Total counts (× 10⁻³)
50
100
150
200
250
Energy (keV)

Fig. 6

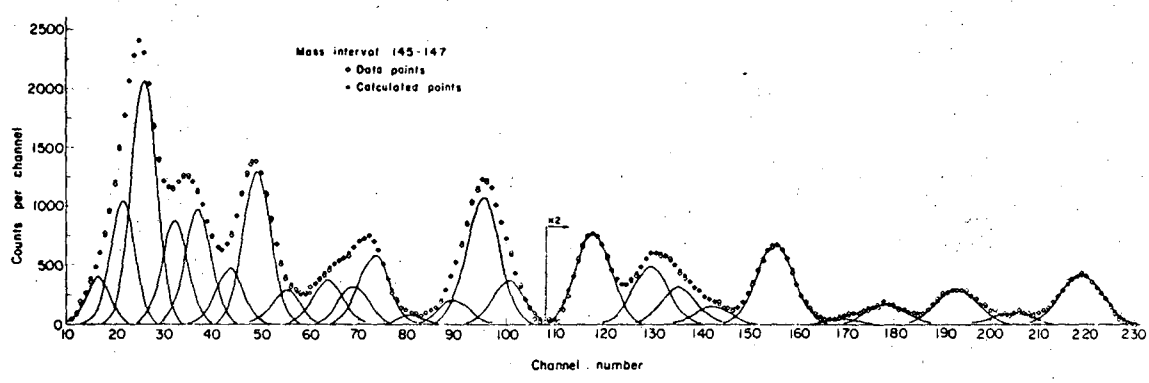
Mass interval 145-147
• Data points
• Calculated points
Counts per channel
Channel number
2500
2000
1500
1000
500
0
10
20
30
40
50
60
70
80
90
100
110
120
130
140
150
160
170
180
190
200
210
220
230

Fig. 7

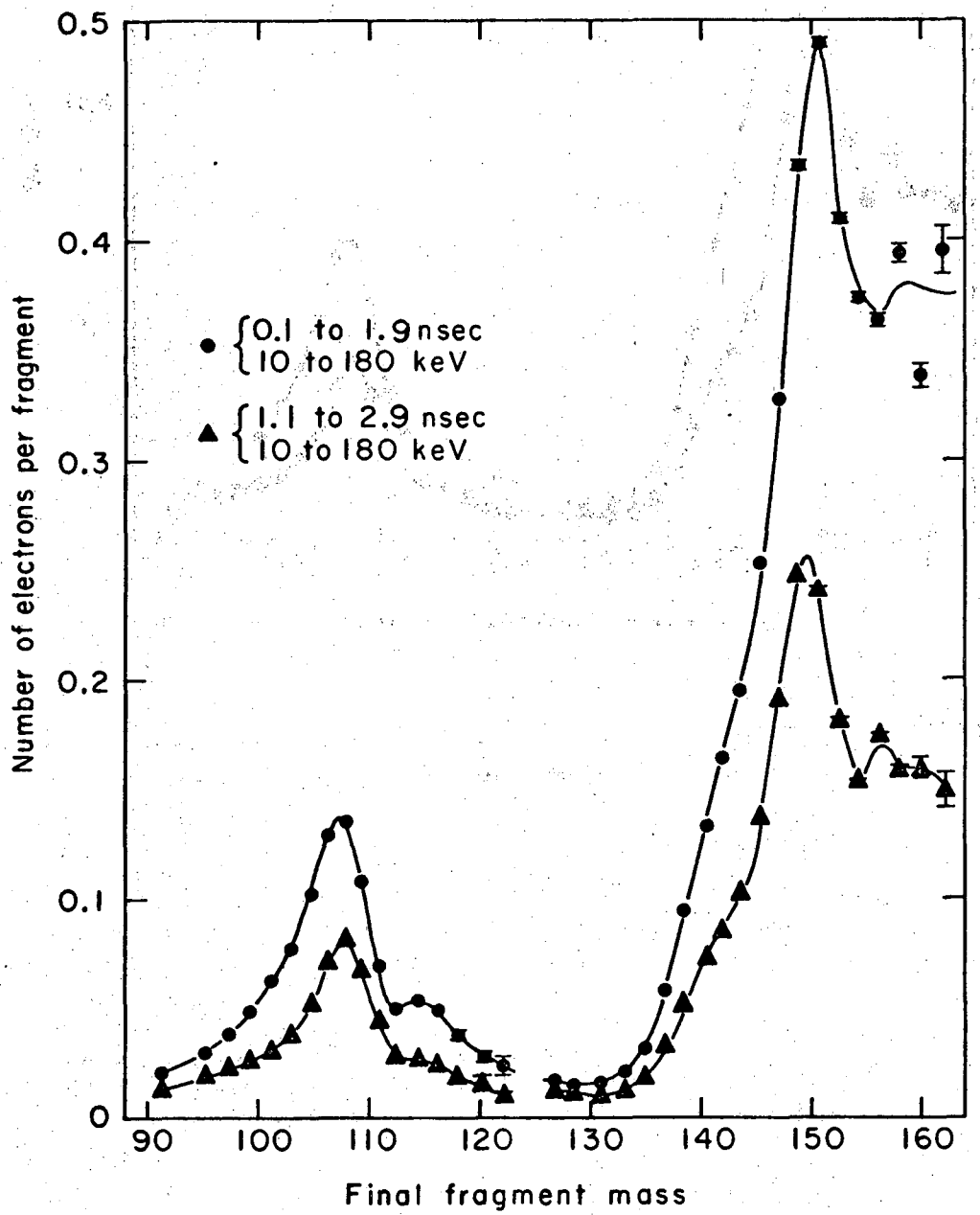

MUB-9906

Fig. 8

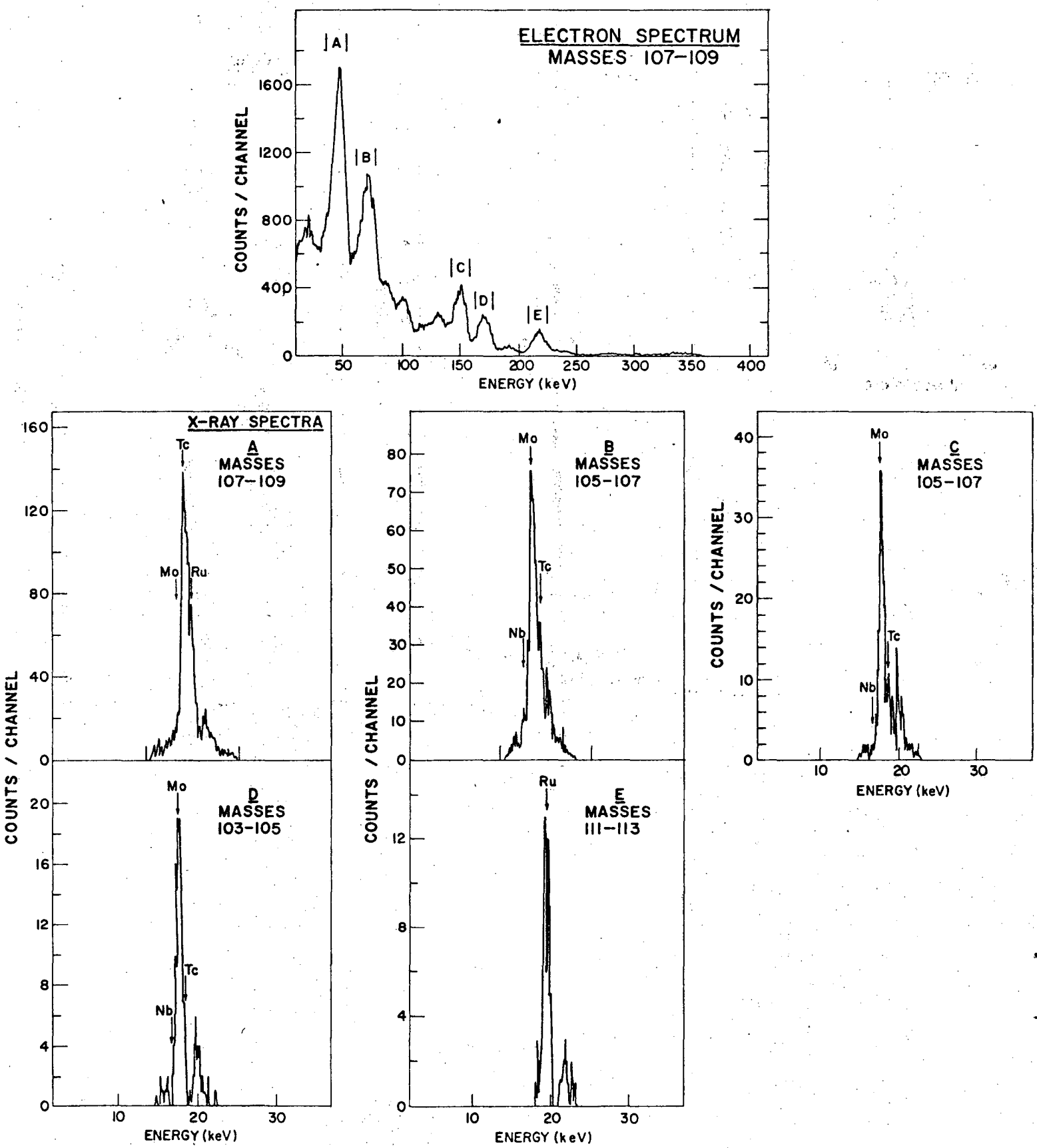
ELECTRON SPECTRUM
MASSES 107–109
COUNTS / CHANNEL
ENERGY (keV)
|A|
|B|
|C|
|D|
|E|
X-RAY SPECTRA
A
MASSES
107–109
Tc
Mo
Ru
B
MASSES
105–107
Mo
Tc
Nb
C
MASSES
105–107
Mo
Tc
Nb
D
MASSES
103–105
Mo
Tc
Nb
E
MASSES
111–113
Ru

Fig. 9

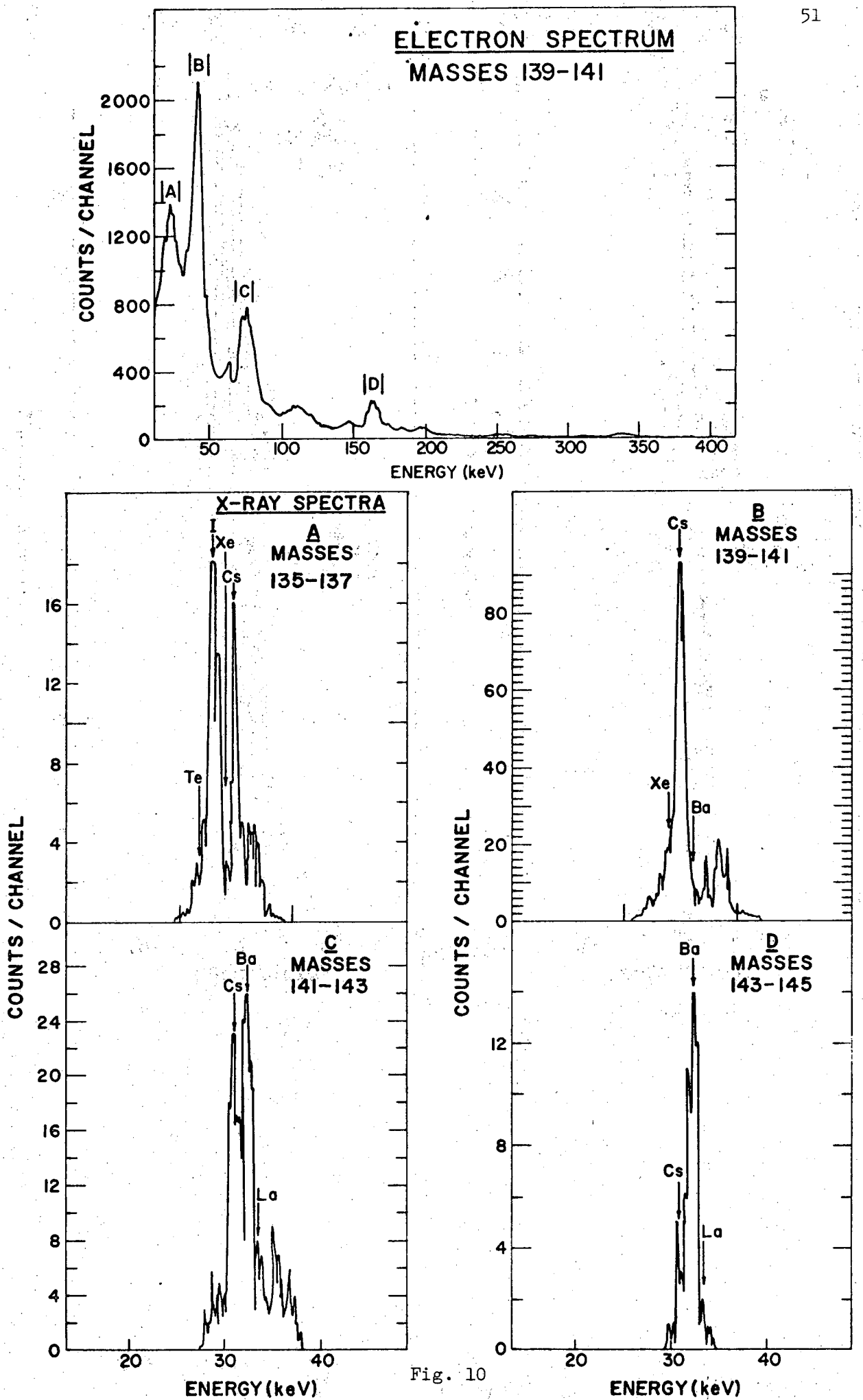
ELECTRON SPECTRUM
MASSES 139-141
COUNTS / CHANNEL
ENERGY (keV)
|A|
|B|
|C|
|D|
X-RAY SPECTRA
A
MASSES
135-137
I
Xe
Cs
Te
B
MASSES
139-141
Cs
Xe
Ba
C
MASSES
141-143
Ba
Cs
La
D
MASSES
143-145
Ba
Cs
La
COUNTS / CHANNEL
ENERGY (keV)

Fig. 10

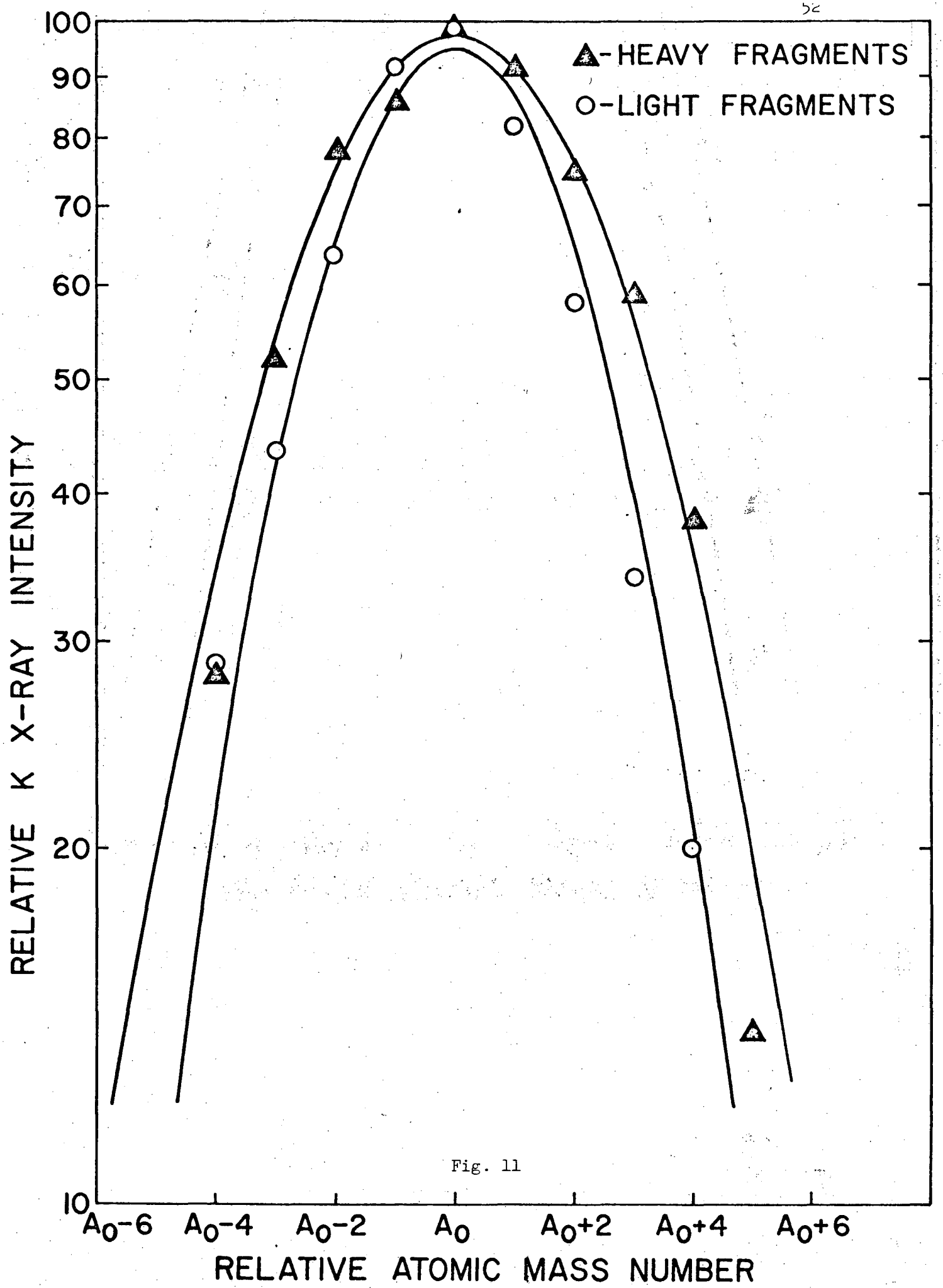
▲-HEAVY FRAGMENTS
O-LIGHT FRAGMENTS
RELATIVE K X-RAY INTENSITY
100
90
80
70
60
50
40
30
20
10
A_0-6
A_0-4
A_0-2
A_0
A_0+2
A_0+4
A_0+6
RELATIVE ATOMIC MASS NUMBER

Fig. 11

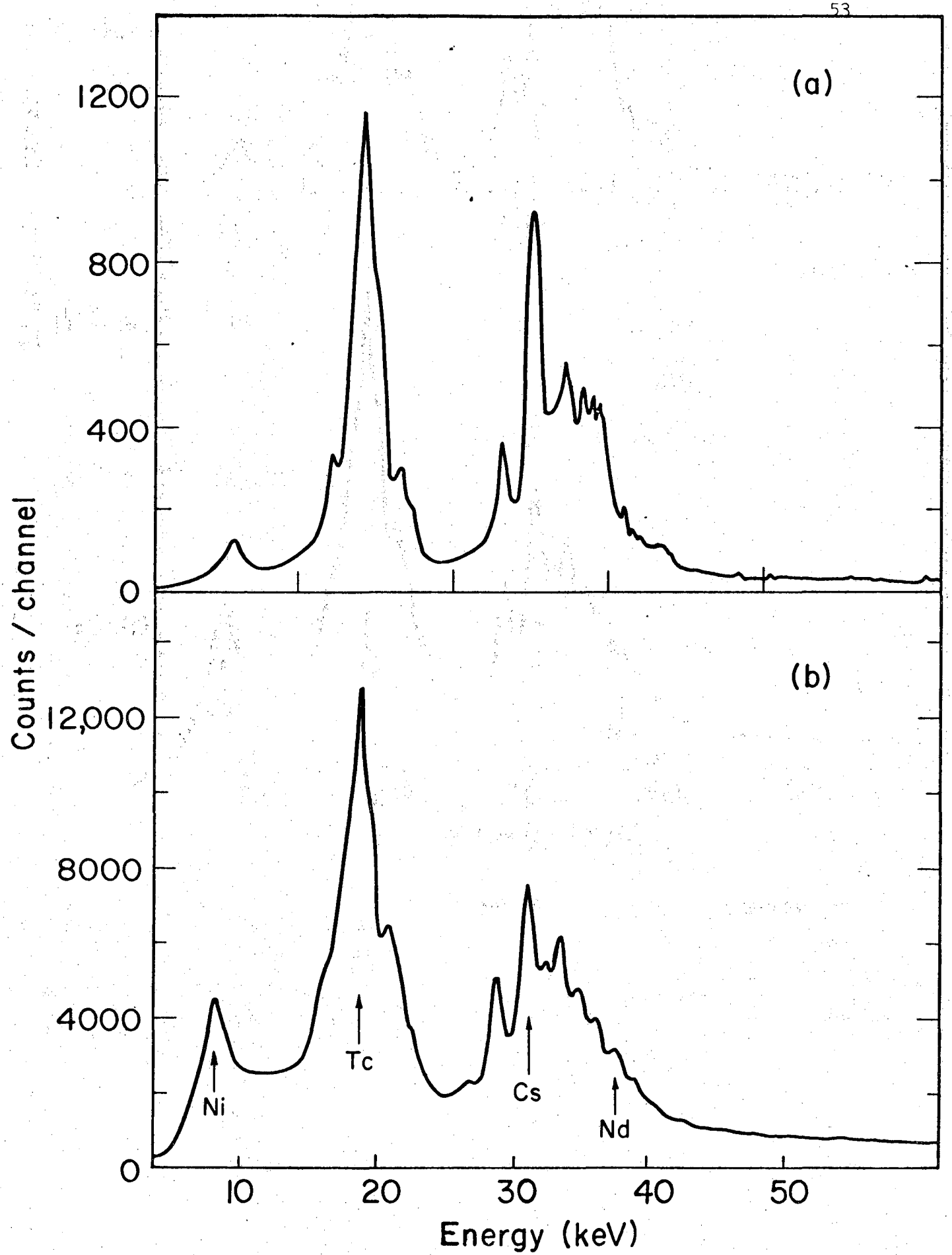

Fig. 12

XBL698-3463

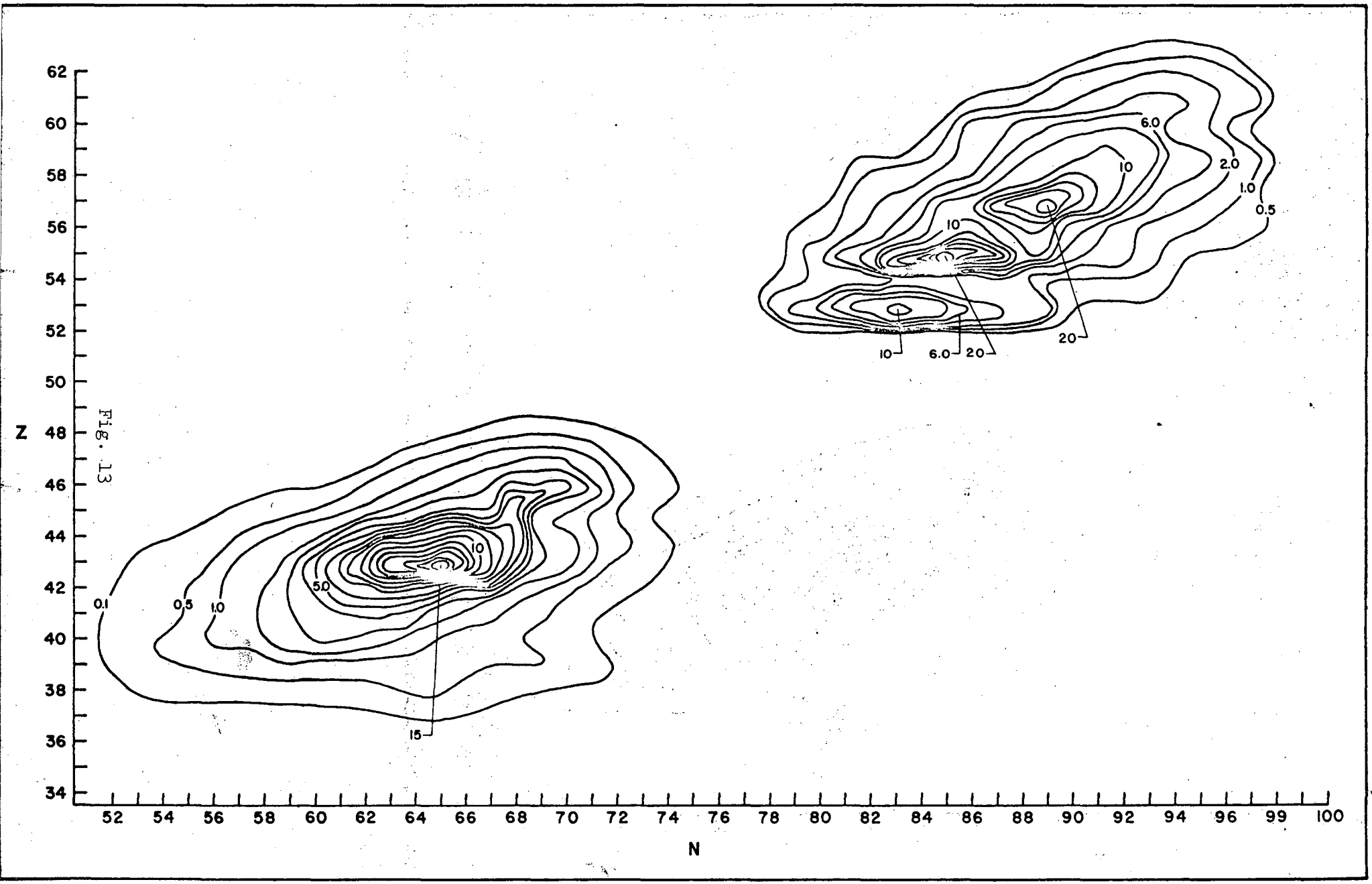
Z
N
62
60
58
56
54
52
50
48
46
44
42
40
38
36
34
52
54
56
58
60
62
64
66
68
70
72
74
76
78
80
82
84
86
88
90
92
94
96
99
100
0.1
0.5
1.0
5.0
10
15
6.0
2.0
1.0
0.5
10
10
6.0
20
20

Fig. 13

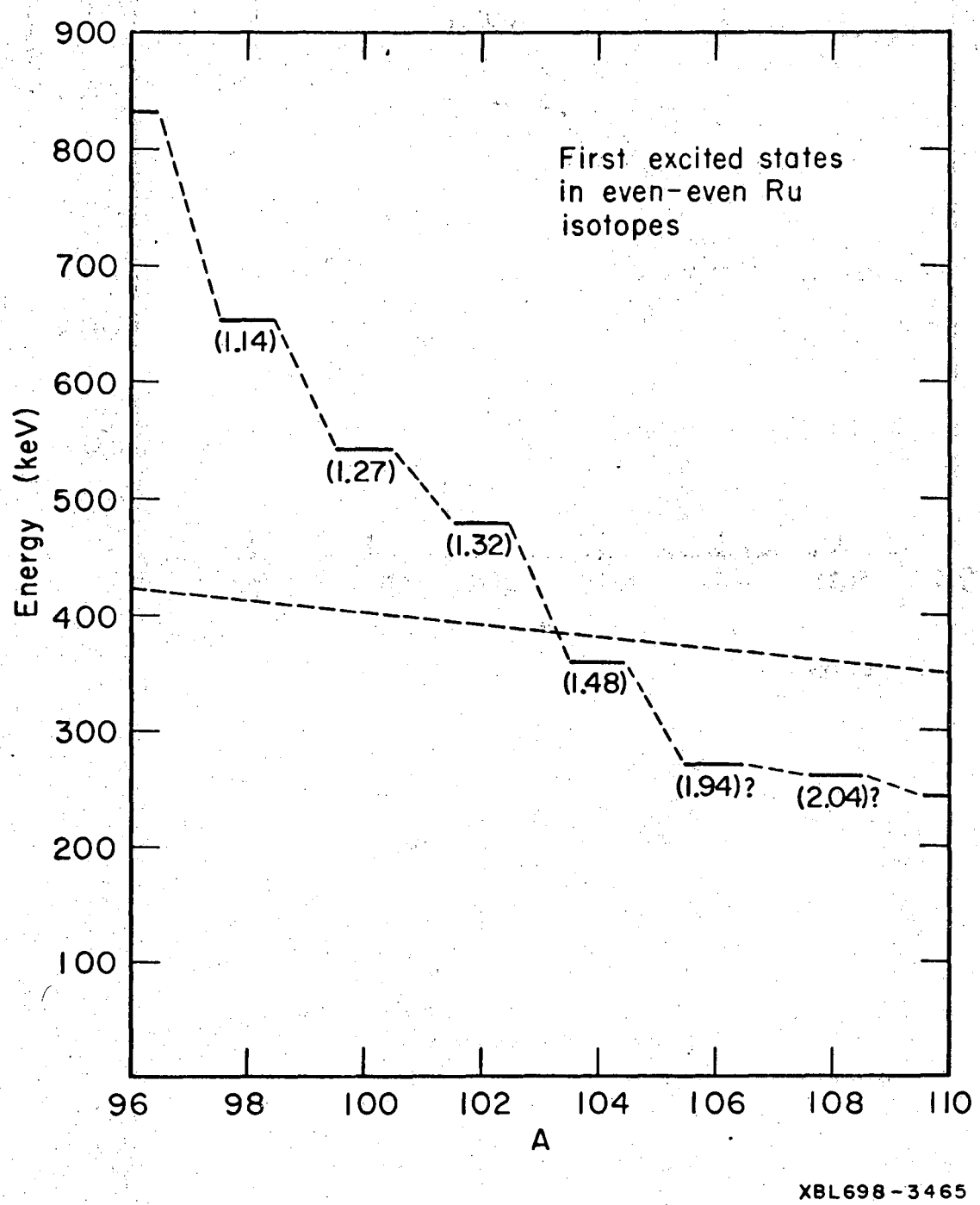
First excited states
in even-even Ru
isotopes
(1.14)
(1.27)
(1.32)
(1.48)
(1.94)?
(2.04)?
Energy (keV)
900
800
700
600
500
400
300
200
100
96
98
100
102
104
106
108
110
A
XBL698-3465

Fig. 14

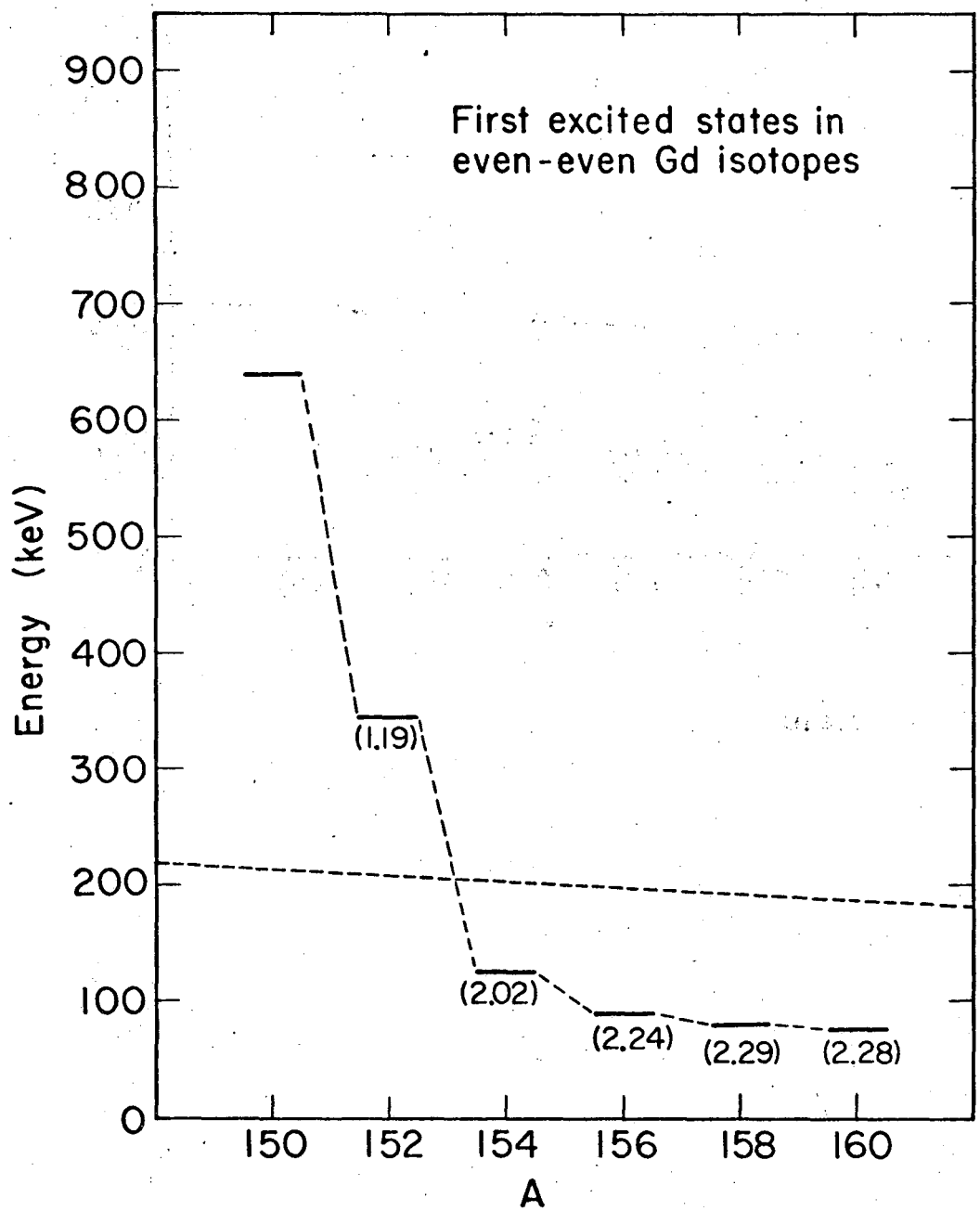

XBL698-3461

Fig. 15

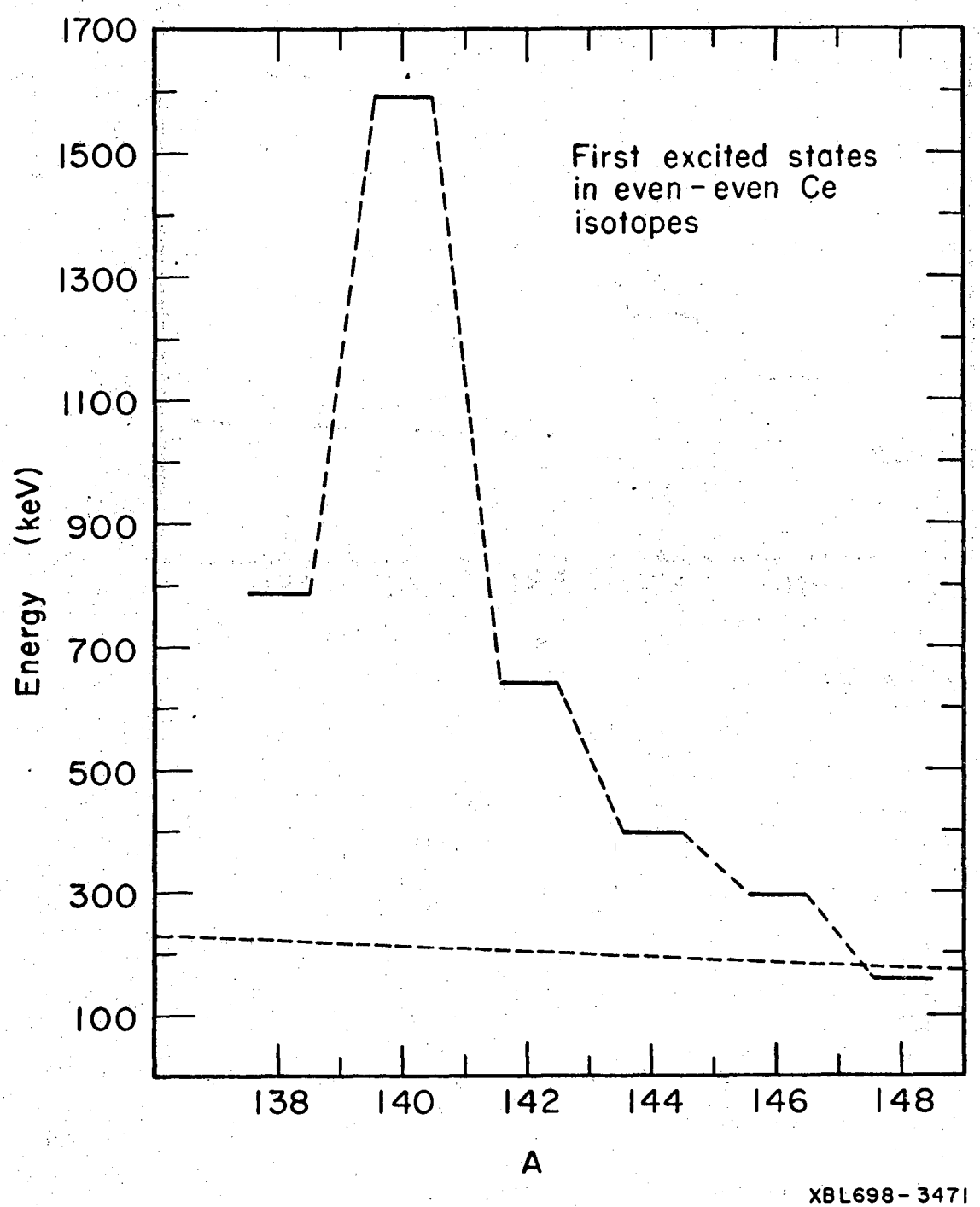
First excited states
in even-even Ce
isotopes
Energy (keV)
1700
1500
1300
1100
900
700
500
300
100
138
140
142
144
146
148
A
XBL698-3471

Fig. 16

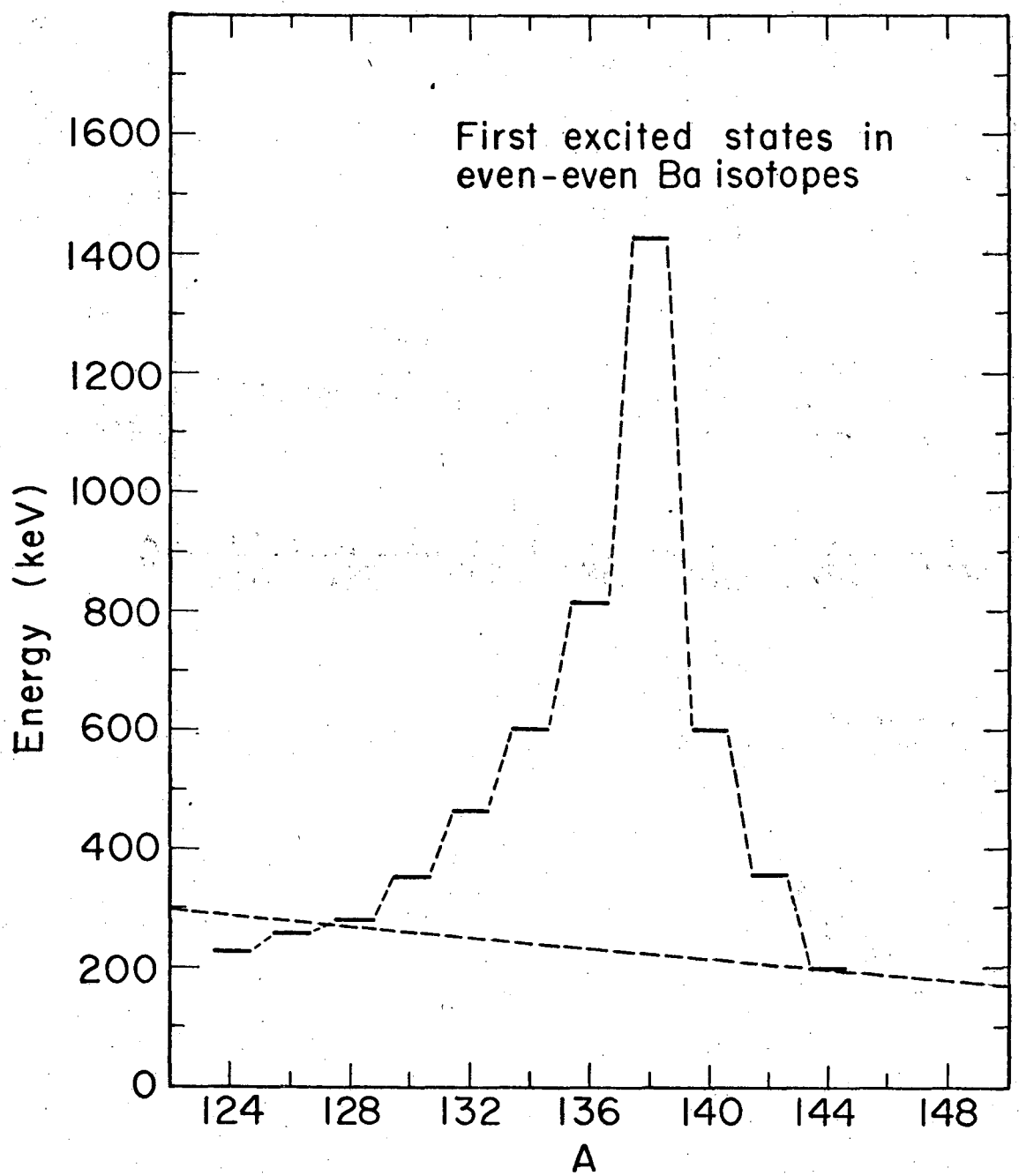

XBL698-3472

Fig. 17

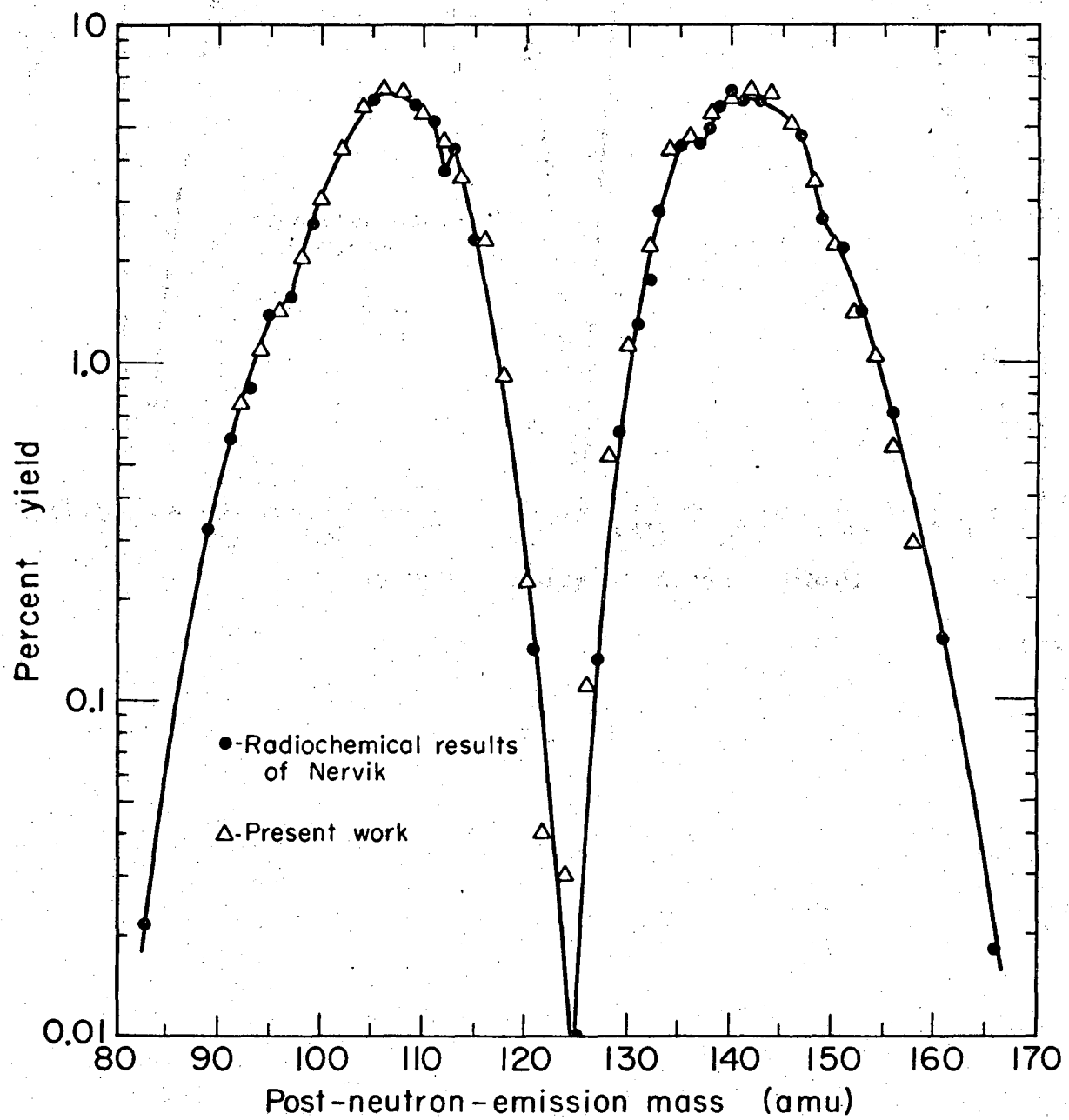

MUB-10853

Fig. 18

LEGAL NOTICE

This report was prepared as an account of Government sponsored work. Neither the United States, nor the Commission, nor any person acting on behalf of the Commission:

A. Makes any warranty or representation, expressed or implied, with respect to the accuracy, completeness, or usefulness of the information contained in this report, or that the use of any information, apparatus, method, or process disclosed in this report may not infringe privately owned rights; or

B. Assumes any liabilities with respect to the use of, or for damages resulting from the use of any information, apparatus, method, or process disclosed in this report.

As used in the above, "person acting on behalf of the Commission" includes any employee or contractor of the Commission, or employee of such contractor, to the extent that such employee or contractor of the Commission, or employee of such contractor prepares, disseminates, or provides access to, any information pursuant to his employment or contract with the Commission, or his employment with such contractor.

TECHNICAL INFORMATION DIVISION
LAWRENCE RADIATION LABORATORY
UNIVERSITY OF CALIFORNIA
BERKELEY, CALIFORNIA 94720